ABSTRACT

THE EXTRACTION OF TYPE I COLLAGEN AND THE FABRICATION OF MULTI-FILAMENT EMBEDDED HYDROGELS FOR GUIDED NERVE REGENERATION

by
Mevan Lakmal Siriwardane

Each year, there are approximately 11,000 new cases of spinal cord injury (SCI) in the United States [2]. There have been some success in pre-clinical studies to induce axonal generation, but the reconnection of axons over large distances remains the greatest challenge. Since the development of nerve conduit to facilitate general axonal regeneration, the primary focus has changed to directing the regeneration of axons while also promoting their outgrowth over very extensive lesions to ensure functional recovery of transected nerves during in vitro experiments by using natural materials such as type I collagen, which is the largest constituent of the extra-cellular matrix of living tissue. In this project, fabrication of novel constructs for nerve tissue guidance was carried out using homogenous hydrogels and multi-filament arrays of wet-spun fibers/hydrogel composites derived from extracted type I collagen. A comparison of axonal outgrowth on 2D and 3D environments revealed that dorsal root ganglia (DRGs) slightly favored 3D collagen gels compared to 2D collagen substrates after 9 days of culture. DRG neurites grown on 3D collagen gels exhibited optimal growth on a 0.8 mg/ml collagen gel concentration.

Extracted type I bovine collagen was wet spun at 2% and 5% wt bovine collagen in ethanol to yield fibers as small as 1.389 μm in diameter. BCA total protein assay and SDS-PAGE were used to validate the quantity and purity of extracted rat tail collagen. Doublet bands present at 235 kDa and 215 kDa and another pair of doublets at 130 kDa

and 115 kDa characteristic of rat tail type I collagen were seen for both extracted and commercial rat tail collagen using SDS-PAGE. Low absorbance values from BCA total protein revealed that this technique is not suitable for quantifying rat tail type I collagen.

**THE EXTRACTION OF TYPE I COLLAGEN AND THE FABRICATION
OF MULTI-FILAMENT EMBEDDED HYDROGELS FOR GUIDED
NERVE REGENERATION**

by
Mevan Lakmal Siriwardane

**A Thesis
Submitted to the Faculty of
New Jersey Institute of Technology
in Partial Fulfillment of the Requirements for the Degree of
Master of Science in Biomedical Engineering**

Department of Biomedical Engineering

January 2008

Blank Page

APPROVAL PAGE

THE EXTRACTION OF TYPE I COLLAGEN AND THE FABRICATION OF MULTI-FILAMENT EMBEDDED HYDROGELS FOR GUIDED NERVE REGENERATION

Mevan Lakmal Siriwardane

Dr. Bryan J. Pfister, Thesis Advisor   Date
Associate Professor of Biomedical Engineering, NJIT

Dr. Cheul Cho, Committee Member   Date
Assistant Professor of Biomedical Engineering, NJIT

Dr. Michael Jaffe, Committee Member   Date
Research Professor of Biomedical Engineering, NJIT

BIOGRAPHICAL SKETCH

Author: Mevan Lakmal Siriwardane

Degree: Master of Science

Date: January 2008

Undergraduate and Graduate Education:

- Master of Science in Biomedical Engineering,
  New Jersey Institute of Technology, Newark, NJ, 2008

- Bachelor of Science in Biomedical Engineering,
  Louisiana Tech University, Ruston, LA, 2006

Major: Biomedical Engineering

Presentations and Publications:

Mevan L. Siriwardane, Holly Martin, Kirk Schultz,
  "A Surface Science Study of Chitosan and Its Use as a Biomedical Implant
  Coating,"
  The 2005 Annual Fall Biomedical Engineering Society (BMES) Conference,
  Baltimore, MD, September 28 – October 1, 2005.

Mevan L. Siriwardane, Holly Martin, Kirk Schultz,
  "A Surface Science Study of Chitosan and Its Use as a Biomedical Implant
  Coating,"
  The Houston Society for Engineering in Medicine and Biology (HSEMB)
  Conference, Houston, TX, February 9 – 10, 2006.

I owe so much to my parents and sister on whose constant encouragement and love I have relied throughout my education. It is to them that I dedicate this work.

ACKNOWLEDGMENT

This work would not have been possible without the support and encouragement of my research supervisor Dr. Bryan Pfister who provided me with valuable and countless resources, insight, intuition, and reassurances. Special thanks are given to Dr. Cheul Cho and Dr. Michael Jaffe for serving on my thesis committee and their advice and input during the preparation of this thesis.

Many of my fellow graduate students Sherry Wang, Fayekah Assanah, and Joseph Loverde of the CHEN Research Laboratory are acknowledged for their assistance in cell culturing and image analysis. I also wish to thank undergraduates Bin Lin and Vivian Ozoko for participation in my research projects during the summer of 2007.

I would also like to thank Dr. Richard Foulds, the director of the Biomedical Engineering Graduate Program for his constant support and guidance. Special thanks are given to Dr. William Hunter, the NJIT Biomedical Engineering Department, and the National Science Foundation (NSF) C2PRISM grant for financial assistance during my graduate studies.

TABLE OF CONTENTS

TABLE OF CONTENTS
(Continued)

Chapter   **Page**

LIST OF TABLES

LIST OF FIGURES

CHAPTER 1

INTRODUCTION

1.1 Motivation

In recent years, there has been tremendous progress in understanding the interactions between biological tissue and materials. The advancements in the emerging field of tissue engineering have offered many therapeutic treatments and new methods in regenerative medicine. However, the progress of tissue engineering approaches in nerve regeneration has been slow and there is much more to be learned about the mechanisms in which various natural and synthetic biomaterials interact with regenerating nervous tissue. Although a few preclinical studies have shown promising techniques that enhance axon outgrowth in animal models of spinal cord injury (SCI), the greatest challenge to overcome is to produce axons of sufficient length and number to completely bridge the extensive lesions seen in SCI.

Approximately 10,000 patients suffering from SCI and another estimated 250,000 have to endure devastating disabilities from chronic SCI each year in the U.S. due to limited techniques available in repairing nerve tissue damage and clinically effective approaches to treat spinal cord lesions [5]. In order to establish effective axon guidance treatments for nerve tissue regeneration, it is desirable to create a nerve conduit for animal studies that naturally mimic the morphology and function of natural axon fascicles. Since type I collagen is a natural component present in most biological tissues, it selected as the central component of the nerve conduit consisting of hydrogel and wet-spun fibers in this study. Type I collagen extracted from bovine tendon was wet-spun into

1

fibers with varying fiber diameters to serve as an extra-cellular matrix (ECM) component of a guided nerve conduit for potentially regenerating dorsal root ganglia axons.

1.2 Background Information: Spinal Cord Injury

Spinal cord injury (SCI) is a severely devastating disorder of the central nervous system (CNS) and often results in the loss of function below the site of injury. In recent decades, more than 60% of spinal cord injuries occurred in patients 15 to 30 years of age, who have still many productive years ahead of them [2]. These injuries to a younger generation of the population impose an enormous healthcare and economic burden on the society. A sudden impact on the spinal cord induces a primary injury site, which consists of severed axons, dying neurons and glia, and a disturbed microvasculature [1]. This primary injury triggers a series of pathological events known as secondary damage mechanisms, which often include vascular and biochemical changes, hemorrhagic necrosis, inflammatory processes and delayed demyelination [1]. These secondary injury mechanisms eventually lead to an extended primary lesion area, which is characteristic of spinal cord injury. Unlike peripheral nerves, the central neuronal pathways of the spinal cord consist of non-regenerating nerve cells that are unable to spontaneously restore synaptic connections. As a result, functional recovery is virtually impossible. Furthermore, dying and degenerating neurons cannot be replaced by new neurons. This cascade of dynamic events results in glial scar tissue proliferation leading to permanent loss of neuronal function and degradation of spinal nerves.

After the initial impact to the spinal cord, these pathological events significantly hinder signal conduction, which is the transmission of action potentials along the length

of axons. This disturbance in signal conduction leads to eventual impairment or loss of body functions, which become mostly permanent. Severed ends of neurons make initial attempts to re-grow but usually fail due to lack of guidance and loss of signal conduction upon injury. Signal conduction can be restored only if regenerating axons reconnect spinal cord circuits. If there is restoration of signal conduction, then the process of functional recovery can be initiated. The restoration of signal conduction is primarily achieved by the regeneration of severed axons and/or the formation of alternative neural pathways. The formation of new nervous system pathways can occur by either, 1) reconnecting severed axons with original target site or 2) establishing an alternate connection with a new site functionally linked to the original target (i.e., wiring around the lesion) [1].

The recapitulation and restoration of neuronal functionality of severed axons occur at a very slow rate due to the hostile environment at the injured lesion site often impeding any chance of central nervous system (CNS) axon re-growth. Severed axon tracts, which are unable to reestablish functional relays, eventually undergo rapid degeneration resulting in permanent loss of neural function. The key factors that seem to act as barriers to axon regeneration are the relative lack of growth promoting factors, presence of growth inhibitory molecules due to inflammatory response, alterations in surrounding extracellular matrix (ECM) vasculature, and the formation of fibroglial scar tissue along with cystic cavities [1]. In this study, the fabrication of a novel nerve conduit will establish the facilitation of spinal axon regeneration by serving as a protective shield from the hostile environment at the injury site.

1.3 Physiology of the Nervous System

A thorough understanding of the physiology of the nervous system is crucial in addressing the challenges of bioengineering research in treating nerve tissue injuries. The application of biomaterials and engineering methodologies in nerve tissue repair requires a broad knowledge of the general organization and the cellular components of the nervous system including the anatomy of the peripheral nerves and the spinal cord.

Organization of the Nervous System. The nervous system is classified into the central nervous system (CNS) and the peripheral nervous system (PNS). The CNS consists of the brain, spinal cord, optic, and olfactory and auditory systems. Many of the functions of the CNS include conducting and interpreting signals in addition to interfacing with the PNS via excitatory stimuli. The PNS consists of cranial nerves from the brain, the spinal nerves from the spinal cord, and the sensory nerve cell bodies (dorsal root ganglia) and their processes. Peripheral nerves innervate muscle tissue, transmitting both sensory and excitatory input to and from the spinal column. In this project, fetal rat dorsal root ganglia were chosen to investigate two- and three-dimensional axonal outgrowth using nerve conduit components made of type I collagen biomaterials.

Cellular Components of the Nervous System. The nervous system is composed of two primary cell types: neurons and neuroglia. Neurons are the basic structural and functional elements of the nervous system and consist of a cell body (soma) and its extensions (axons and dendrites). In this study, the axons and their outgrowth/regeneration behavior is the primary focus. Clusters of sensory nerve soma, known as ganglia, are located just outside the spinal column. While dendrites transmit

electrical signals to the neuron cell body, the axon conducts impulses away and to other neighboring neurons with dendrite receptors. Glial cells, or neuroglia, are supporting cells that aid the function of neurons and are present in both PNS and CNS. Neuroglia include Schwann cells in the PNS and astrocytes and oligodendrocytes in the CNS. The formation of glial scar tissue caused by the accumulation of astrocytes and oligodendroctyes during SCI or other CNS injuries provides a hostile environment for the regenerating axons. Glial cells, unlike neurons, are more abundant and exhibit some capacity for cell division. Although neurons cannot divide by mitosis, they can regenerate a severed portion or sprout new neural branches under certain limited conditions.

In the PNS, sheaths of living Schwann cells surround all axons. On the outer surface of this inner Schwann cell layer is the neurilemma, which is a basement membrane similar to that found in epithelial layers. Unlike the axons in the PNS, CNS axons do not have this continuous protective basement membrane and sheath of Schwann cells. Many axons in the CNS are only surrounded by an insulating myelin sheath, which is formed from dense layers of successive wrappings of oligodendrocytes. Myelin serves to increase the propagation velocity of the nerve impulse, which becomes especially important for axons with extensive lengths (up to 1 m).

Anatomy of the Peripheral Nerve and Spinal Cord. In the context of designing nerve conduits for facilitating guided nerve regeneration, a firm background knowledge of peripheral nerve and spinal cord anatomy is essential. A peripheral nerve consists of motor and sensory axons bundled together by support tissue into an anatomically defined nerve trunk exhibiting a hierarchical level of structural organization (Figure 1.1). The perineurium, which is formed from many layers of flattened cells and collagen, surrounds

groups of axons to form bundle-like fascicles. The epineurium is the outermost sheath of loose fibrocollagenous tissue, and it binds individual nerve fascicles into a nerve trunk. Peripheral nerves are well vascularized by capillaries within the support tissue of the nerve trunk or by vessels that penetrate the nerve from surrounding arteries and veins. A thin encapsulating layer called an endoneurium surrounds individual axons and their Schwann cell sheaths and is mainly composed of oriented collagen fibers. Therefore, type I collagen was selected during this study to fabricate nerve conduit materials consisting of collagen gels and wet-spun collagen fibers as the main structural component.
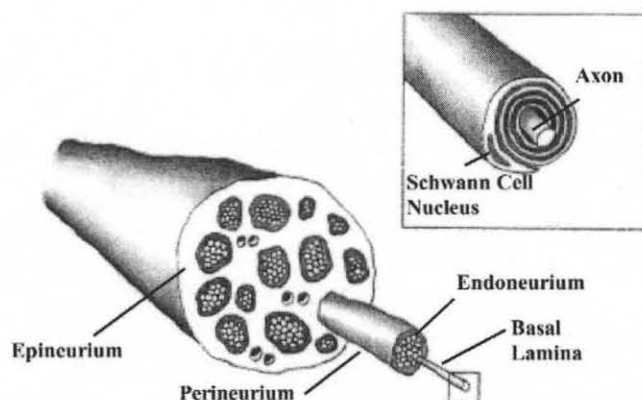
Figure 1.1 Anatomical structure of the PNS [4].

The spinal cord is composed of dendrites, axons, and cell bodies (Figure 2). In the center of the spinal cord is a butterfly-shaped region referred to as gray matter, which contains the cell bodies of excitatory neurons including glial cells and blood vessels.

The gray matter is surrounded by white matter, which helps to protect and insulate the spinal cord. White matter consists of axons and glial cells, including

oligodendrocytes, astrocytes, and microglia (immune cells). In the CNS, the oligodendrocytes serve to myelinate the axons in the CNS while the astrocytes contribute to the blood-nerve barrier, which separates the CNS from blood proteins and cells. Axons project from the white matter in bundles, known as fascicles, which extend to the encasing bone of the spinal column, travel through the PNS-CNS transition zone, and enter the PNS.

[4]
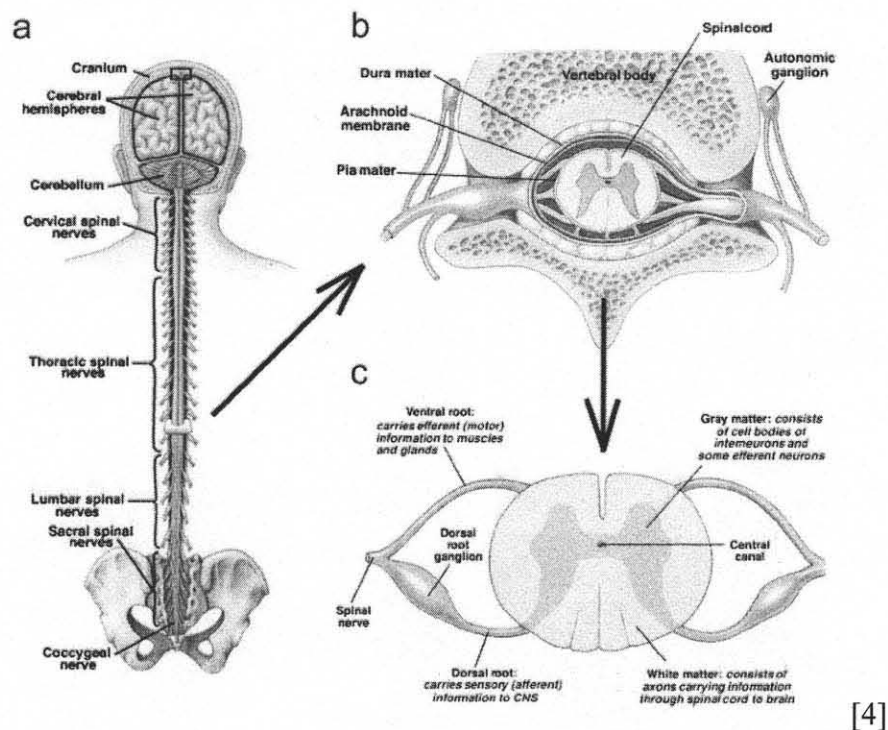
Figure 1.2 Anatomy overview of the spinal cord. (a) Spinal cord consists of the cervical, thoracic, lumbar, sacral, and coccygeal spinal regions. (b) Nerves are well protected by vertebrae and protective membranes. (c) The nerves on left and right side are subdivided into roots.

1.4 Nerve Injury and Regeneration

<u>Peripheral Nervous System.</u> The most severe injury to the PNS is a complete nerve transection. After a nerve is severed, the distal portion begins to degenerate as a result of disrupted protein transport and separation from the metabolic resources of the nerve cell

bodies. The cytoskeleton begins to breakdown, followed by the dissolution of the cell membrane. The proximal end of the nerve stump swells, but experiences only minimal damage via retrograde degradation. During the onset of cytoskeleton and membrane degradation, Schwann cells surrounding the axons in the distal end shed their myelin lipids. Phagocytotic cells, such as macrophages and Schwann cells, clear myelin and axonal debris. In addition to clearing myelin debris, macrophages and Schwann cells also produce cytokines, which enhance axon growth. Following debris clearance, regeneration begins at the proximal end and continues toward the distal stump. New axonal sprouts usually emanate from the nodes of Ranvier, nonmyelinated areas of axons located between Schwann cells. Functional reinnervation requires that axons extend until they reach their distal target, and in humans, axon regeneration occurs at a rate of about 2–5 mm/day. As a result, significant injuries can take several months to heal.

Central Nervous System. A key difference between the PNS and CNS is the capacity for peripheral nerves to regenerate unlike CNS axons, which do not regenerate appreciably in their native environment. Several glycoproteins in the native extra-cellular environment (myelin) of the CNS are inhibitory for regeneration. The physiological response to injury in the CNS is also different compared to that of the PNS. After injury in the CNS, macrophages infiltrate the site of injury much more slowly compared to macrophage infiltration in the PNS, delaying the removal of inhibitory myelin. This is largely a result of the blood-spine barrier, which limits macrophage entry into the nerve tissue to just the site of injury, where barrier integrity is weakened. In addition, cell adhesion molecules in the distal end of the injured spinal cord are not upregulated appreciably as they are in the PNS, limiting macrophage recruitment. Finally, astrocytes proliferate in a manner similar

to that of Schwann cells in the PNS, but instead become "reactive astrocytes," producing glial scar tissue that inhibits regeneration.

1.5 Collagen Overview

The collagens comprise of a family of fibrous proteins found in all multicellular animals. Since collagen is biodegradable, biocompatible, and nonimmunogenic, it is a desirable material for a variety of biomedical applications. Collagen is the most abundant protein in the tissues of vertebrates and is present in at least ten different forms, each of which is dominant in specific tissue. As one of the major components of the extra-cellular matrix (ECM), collagen is well known to promote cellular proliferation and tissue healing. The commonality among all the types of collagen is the characteristic triple helix, which consists of three left-handed α-helices wound into a right-handed triple helix (Figure 3). Each individual α-helix chain contains one or more polypeptide sequences (Gly-X-Y), in which X and Y positions are frequently occupied by proline and hydroxyproline residues, respectively.
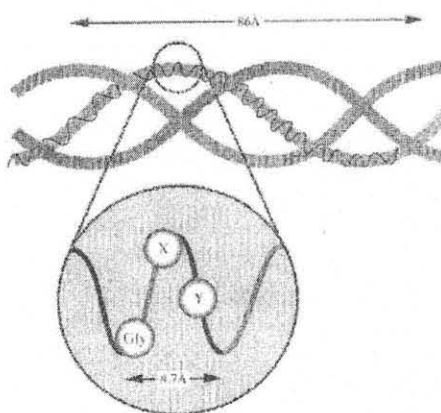
Figure 1.3 Collagen triple helix

Glycine constitutes about one-third of all residues while proline and hydroxyproline make up about 13% and 10%, respectively. The variations within this triple helix are limited to the length of the helix and the number of carbohydrate attachments on the triple helix contributing to all the different structural types of collagen. The different α-chains that constitute the collagen triple helix associate with each other in the following manner:

1) Hydrogen bonding between the NH group of glycines and the CO group from residues of the other α-chains.

2) Hydrogen bonding among OH groups of hydroxyprolines.

3) Hydrogen bonding with water molecules.

These bonds are essential for stabilizing the triple-helical structure of collagen. The repulsion from proline residues is the key factor in contributing to the helical structure and turns the H-side chain of the glycines to the inside of the helix. All the bulky side chains point to the outside of the collagen triple helix due to the lack of space inside the helix. In general, glycines, prolines, and hydroxyprolines are the primary residues responsible for maintaining the triple helix structure while the remaining amino acid residues play key roles in higher order structural regularities. The amino acid residues 4- and 3-hydroxyproline and 5-hydroxylysine are almost exclusively found in collagen and are vital for interchain linking with hydrogen bonds for stability of the helical structure. As a result, the stability of the collagen triple helix strongly depends on the delicate proportion of prolines and hydroxyprolines.

The structure of the α-helix chains is often used to classify collagen into fibrillar and nonfibrillar forms. The fibrillar collagens comprise of types I, II, III, V, and XI. These collagen types form distinct cross-striated fibrils, and all share a triple helical region containing approximately 1,000 amino acids per chain, which has a length of about 300 nm. These different structural forms of collagen contribute to their varying composition from one tissue to another. The structural nature of type I collagen enables it to form fibrils unlike some of the other nonfibrillar types of collagen. As a result, type I collagen is found in tissues such as skin, tendon, ligaments, and bone where mechanical strength and tensegrity are important factors in tissue function. While type I collagen is the primary constituent that makes up the extra-cellular matrix (ECM) of most biological tissue, it is also broadly used for supporting nerve growth. Therefore, type I collagen was the material of choice for this experiment.

There are various sources that can be used to extract type I collagen. The main sources of collagen for commercial applications are bovine tendons, calf, or pig hide. In general reconstituted collagen products are prepared *in vitro* by purification of native collagen by enzyme treatment and chemical extraction. Once the collagen is purified, it can be dispersed or dissolved in solution, filtered, and retained. Furthermore, purified collagen can also be reconstituted into fiber, film, or sponge form through extrusion, casting, or lyophilization techniques.

In this study, dialysis procedures were performed on the material as part of the extraction process to assure purity while the final form of the material was reached only after lyophilization. Type I collagen was extracted from two sources: rat tail tendon and bovine tendon. In the case of rat tail collagen, the end product was a sponge-like material

with the use of lyophilization. Since bovine samples are the most readily available and generate a huge yield per tendon, they are the most ideal to use as a source of type I collagen. The end product following lyophilization of bovine collagen was interwoven fibrous string-like material. In this study, dorsal root ganglia (DRG) neurite outgrowth behavior on rat tail and bovine type I collagen was investigated. A SDS-Page was used to identify the level of purity of the type I collagen and to check for any other protein contamination.

1.6 Challenges and Bioengineering Strategies for Nerve Repair

Although there have been tremendous progress in nerve repair therapies such as the nerve graft, there still remains a strong demand for more clinically approved therapies. In the PNS, an alternate approach to autologous nerve grafts is desired. Some alternative treatments that have been developed in the recent years include nerve guidance channels, especially for more extensive lesions. In the CNS, there are greater challenges encountered for developing new therapies. Research in the area of spinal cord injury (SCI) remained stagnant until a 1980 study revealed that spinal nerves were able to regenerate [4]. In some studies, embryonic spinal cord grafts and peripheral nerve tissue grafts have been shown to support regenerating axons in the CNS but with limited success in guiding them to specific targets [4]. Therefore, many bioengineering efforts are focused on creating a permissive environment for regeneration while providing a means of guiding regenerating axons to establish functional recovery with the damaged nerve ends. Many researchers are currently focusing on efforts to create physical or chemical pathways for regenerating axons. Some latest approaches include physical or

mechanical guidance cues, cellular components, and biomolecular signals. Perhaps, future therapies will incorporate multiple cues in an integrated bioreactor device that more closely mimics native tissue.

CHAPTER 2

CURRENT TECHNIQUES FOR NERVE REPAIR

2.1 Autologous Tissue Grafts

For several decades, autologous tissue grafts have been the gold standard for repair of a peripheral nerve defect. Since they are natural materials, autologous tissue grafts possess several advantages and are more likely to be biocompatible compared to synthetic, artificial materials. In addition, they have been shown to be less toxic and provide a suitable support structure to promote cell adhesion and migration. The potential difficulties that arise with autografts include isolation and controlled scale-up [4].

In recent years, autologous tissue grafts have been used extensively for nerve repair applications. The sources of nerve autografts are typically derived from one of several cutaneous nerves, such as the sural or saphenous nerve. These nerves have an available length up to approximately 40 cm and a cable diameter of 2-3 cm [4]. For peripheral nerve injury, treatment typically consists of either direct end-to-end surgical reconnection of the damaged nerve ends (Figure 3) by the use of an autologous nerve graft. However, suturing the two nerve ends together can only repair small defects or gaps in the nerve. For longer nerve gaps, this approach is not desired because any tension introduced into the nerve cable would inhibit nerve regeneration.

In addition to the autologous nerve graft, other natural tissues such as autologous muscle and vein grafts have been employed but with limited clinical success. In terms of peripheral nerve repair, epineurial sheaths, tendon grafts, muscle-vein grafts, and vein grafts impregnated with autologous Schwann cells are just a few examples of the research

efforts focused on natural tissue grafts.
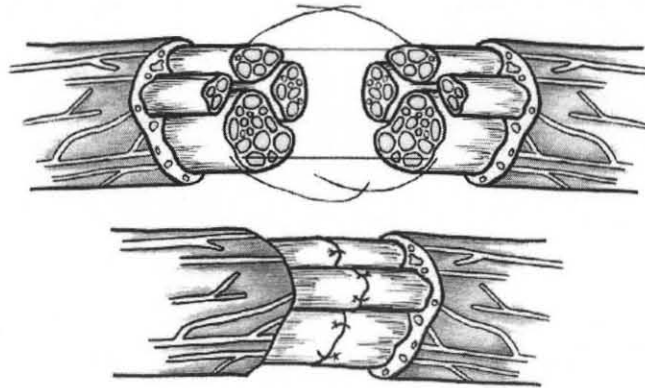
Figure 2.1 Surgical end-to-end reconnection [4].

Despite the encouraging results in research, there still remains a series of drawbacks to using autologous tissue grafts. Since an autologous nerve graft must be harvested from another site in the body and then used to span the injury site, this approach is not practical for a larger nerve defect. In addition, there are many disadvantages to using autologous nerve grafts such as loss of function at the donor site and the need for multiple follow-up surgeries [4].

2.2 Nonautologous Tissue and Acellular Grafts

Since there have been many limitations with using autologous tissue as nerve grafts, the use of nonautologous tissue and extracellular matrix (ECM)-based materials have become the focus of intense research. Allogenic and xenogenic tissues (donor tissue from cadavers and animals, respectively) provide many benefits such as an abundant supply while not having to harvest tissue from the patient. Nevertheless, tissues from these sources exhibit a potential risk for transmitting disease and eliciting an immune response.

In order for these tissues to be biocompatible for nerve conduit applications, they must be used in conjunction with immunosuppressants or they must be acellular (immunogenic components and cells removed).

The decellularization of tissue is considered effective when all immunogenic cellular components are removed while leaving the structure of the ECM well intact. Some techniques used to decellularize nonautologous tissue include thermal decellularization, which involves repeated freeze-thaw cycles to kill and fragment cells. Although this technique appears to be effective in minimizing immune response, there is no guarantee that all cellular remnants are completely removed. Radiation treatments are also used to destroy cells in tissues but also fail to extract all cellular components. Although acellular tissues for clinical nerve repair may be a viable option in the future, better decellularization techniques are needed.

Some other natural nonautologous tissues investigated for neural tissue engineering applications include small intestinal submucosa (SIS) and amniotic tissue grafts [4]. SIS is extracted from the mucosa and muscle layers of the small intestine, which are rinsed in hypotonic solution to lyse and wash away cells. Once SIS is processed, the resulting ECM material consists of collagen, fibronectin, growth factors, glycosaminoglycans (GAGs), proteoglycans, and glycoproteins, which are all conducive to cell adhesion, cell growth, and cell differentiation [4]. Therefore, SIS tissue grafts may be a potential alternative to nerve autografts. Amnion obtained from human placental tissues has also been heavily explored for its potential use in nerve regeneration applications. Amnion tissue is processed by the removal of the epithelial cell layer while preserving the structural integrity of the basement membrane and stromal surfaces. The resulting

acellular amnion tubes may demonstrate potential for nerve regeneration given further studies to validate its application as a nerve conduit.

2.3 Natural-Based Materials

Besides using intact ECM acellular tissues, there have been tremendous research interests in the use of purified natural ECM proteins, proteoglycans, and glycosaminoglycans, which can be modified to serve as appropriate scaffolding for nerve repair and regeneration. Many studies have revealed that ECM molecules such as laminin, collagen, and fibronectin play significant roles in neuron adhesion, axonal development, and nerve repair in the body [9, 16-18]. Many of these ECM component molecules provide chemical and physical cues, which are factors that can modulate neural activity and enhance neurite outgrowth. ECM proteins laminin, fibronectin, and collagen have been used as coatings, filaments, matrices, and hollow tube conduits in numerous nerve repair applications [9-12, 14, 16-18]. In other studies, collagen tubes containing a porous collagen-glycosaminoglycan matrix have demonstrated nerve regeneration rates comparable to nerve autografts [4].

In addition to ECM molecules, other naturally derived molecules that have been studied include fibrinogen, hyaluronic acid, fibrin gels, self-assembling peptide scaffolds, agarose, alginate, and chitosan. The research focus in many latest studies is to further modify these materials through photolithographic patterning techniques or by combining them with other bioactive molecules or growth factors to further enhance neurite extension. Although there have been many experimental successes with these natural materials, very few approaches have been clinically approved.

2.4 Synthetic-Based Materials

Many synthetic materials have also been investigated for nerve repair applications. There are many advantages to using synthetic materials because their chemical and physical properties (i.e., mechanical strength, porosity, degradation rate) can be specifically optimized for any given application. Synthetic materials pose challenges in biomedical applications because the body's inflammatory response can vary considerably from one material to another. In some cases, certain synthetic materials are tolerated by the body's immune system but are incompatible with cell adhesion and tissue repair.

The choice of a synthetic material should be heavily evaluated to ensure the material meets specific criteria for the intended biomedical application. Synthetic materials that are intended for nerve repair applications should possess the following desired properties:

- Easily shaped and formed to desired dimensions

- Sterilizable

- Biodegradable

- Non-toxic/Nonimmunogenic

Synthetic materials that remain permanent are more inclined to provoke a chronic inflammatory response. Nerve guide conduits with materials that degrade as the nerve regenerates are most desirable. A number of different synthetic materials have been explored for use in aiding nerve regeneration such as poly(glycolic acid) (PGA), poly(lactic acid) (PLA), and poly(lactic-co-glycolic acid) (PLGA). They are classified as poly(esters) and have been processed as foams or scaffolds or seeding with Schwann

cells to enhance regenerative potential in several studies. These materials continue to be studied and further modified for nerve repair applications due to their availability, ease of processing, biodegradation characteristics, and FDA approval.

Many studies have also used nondegradable synthetic materials such as silicone for nerve conduits. Although silicone tubes can be used to bridge short gaps with some success, they do not support regeneration across defects larger than 10 mm unless growth factors are incorporated [4]. Furthermore, the impermeable and inert properties of silicone tubes limit their application as nerve conduits. As a result, a great deal of research is now focused on developing semipermeable or degradable guidance channels that can facilitate regeneration over more extensive lesions.

Poly(ethylene glycol) (PEG) has also been applied to nerve regeneration applications. In one study, PEG was the material of choice for fusing the membranes of severed nerve ends from sciatic and spinal nerves [4]. However, the limitation of this approach is that it can only be applied for small nerve defects in which the severed nerve ends are directly adjacent to each other. Other efforts have focused on using cross-linked PEG hydrogels that are modified with factors to mimic the ECM [4].

2.5 Cellular-Based Therapies

Nerve regeneration can be facilitated by the application of vital biomolecules such as supportive ECM components, neurotrophic factors, and cell adhesion molecules. Cells are essential in any tissue engineering or reparative medicine approach since they are carriers and producers of many of these vital biomolecules. Glial cells such as Schwann cells, astrocytes, and oligodendrocytes along with other cells like macrophages support

nerve tissue regeneration by clearing debris and secreting neurotrophic factors to aid axonal outgrowth [4]. Some other cells including stem cells and genetically modified cells have been intensely studied as grafts for supporting nerve regeneration.

Schwann cells, which are one of many types of glial cells are primarily responsible for the supportive environment within nerve tissue since they produce the extra-cellular matrix (ECM), cell adhesion molecules, integrins, and neurotrophins. Schwann cells are also intensely studied for nerve regeneration because they are known to play a critical role in leading peripheral axons to the distal nerve stump. A series of studies of Schwann cells in central and peripheral nerve injuries have primarily focused on techniques to deliver these cells to the injury site [4]. However, there are several challenges facing Schwann cell therapies for spinal cord repair. Regenerating axons that grow into Schwann cell grafts often fail to leave this favorable environment due to harsh interactions with components in glial scar tissue. Furthermore, Schwann cells have not been found to remyelinate axons beyond the injury site and may actually increase chondroitin sulfate proteoglycan, which is a non-permissive component of glial scar. Although Schwann cells have been associated with some success in promoting spinal cord repair, they may show more promise when combined with other treatments

Glial cells such as astrocytes, oligodendrocytes, and microglia as cell-based therapies still remain to be well understood. There may be limitations in using CNS glial cells since they are capable of contributing to the formation of glial scar tissue, which is inhibitory toward axonal growth. Therefore, a greater understanding of CNS glia must be obtained before dependable therapies can be implemented for spinal cord repair.

Macrophages, like Schwann cells, play a vital role in promoting peripheral nerve repair by removing myelin debris. Therefore, many researchers have transplanted macrophages into peripheral nerve and spinal cord injuries [4]. Macrophage-based transplants have been associated with a significant decrease in myelin-associated glycoproteins while increasing axonal regeneration. Although macrophages are known to clear myelin debris at a nerve injury site, other means by which they aid in regeneration remains unclear.

Many researchers have recently investigated the potential of stem cells in nerve regeneration applications. Neural stem cells have been isolated from rodent brain, spinal cord, skeletal muscle, and bone marrow [4]. For example, stem cells implanted in an injured rat spinal cord have survived and were able to differentiate into neurons, astrocytes, and oligodendrocytes. Furthermore, other studies have also found that stem cells implanted into an injured spinal cord differentiate into neurons and glial cells [4]. The greatest challenge is providing an environment conducive to stem cell differentiation into specific neural lineages to yield more predictable results. Although glial progenitors have been used successfully in remyelination applications, their use as a therapy following spinal cord injury remains to be understood [4].

Transplanted genetically modified cells, are another cell-based therapy that pose advantages as a means to deliver a continual supply of active growth factors for nerve regeneration such as neurotrophins. If gene expression in modified cells can be turned on and off, it is possible that expression of nerve growth factors could be directed in a complex manner conducive to nerve regeneration. For example, genetically modified fibroblasts have been a highly studied model for the delivery of neurotrophins. In many

studies, fibroblasts have been engineered to produce NGF, BDNF, NT-3, CNTF, GDNF, and bFGF [4]. Implants of transfected fibroblasts have provided information regarding the application of active neurotrophins locally to the nerve injury site. More advanced studies have included a molecular "on switch" to control the genetically modified expression of NGF in fibroblasts. Despite the advancements in cell-based therapies for tissue engineering applications, future studies are vital in making them more applicable to nerve repair and spinal cord injury.

CHAPTER 3
MATERIAL AND EXPERIMENTAL METHODS

This project was conducted to investigate the axon outgrowth behavior of fetal rat dorsal root ganglia (DRG) on 2D and 3D environments composed of type I collagen from either rat tail tendon or bovine tendon. During this study, a detailed extraction protocol was established for the extraction of type I collagen from rat tail tendon. The validity of this extraction protocol was analyzed through cell culture studies and protein assay techniques that will be discussed in further detail in this chapter. Furthermore, it is desirable to determine if type I collagen can be wet-spun into multi-filament fibers tailor-made as a guiding platform for growing DRG axons cultured *in vitro*. The results of DRG explant behavior on the collagen substrates will be used to determine suitable structural material components for a nerve guide conduit as a treatment methodology for SCI.

3.1 Collagen Extraction Process

The protocol for type I collagen extraction from rat tail tendon was compiled from a series of previous extraction techniques. The rat tail tendons were obtained from euthanized female rats at the Rutgers-Newark Animal Facility. The tendon from severed rat tails were utilized for the extraction of type I collagen. The age of the rats used for this extraction process varied from 4-6 months.

The rat tails obtained from 10 female rats were stored on ice for 10-15 minutes during transport to the NJIT CHEN facility for further processing. They were thoroughly rinsed and scrubbed in antiseptic soap/water and 80% alcohol for sterilization purposes. Then, the rat tails were rinsed in sterile distilled reverse osmosis water. Once the

cleaning process was complete, the tails were stored on filter paper in Petri dishes and frozen for 24 hours. On the following day, the tails were once again sterilized in an 80% alcohol immersion for 15 minutes and then air-dried for 5 minutes.
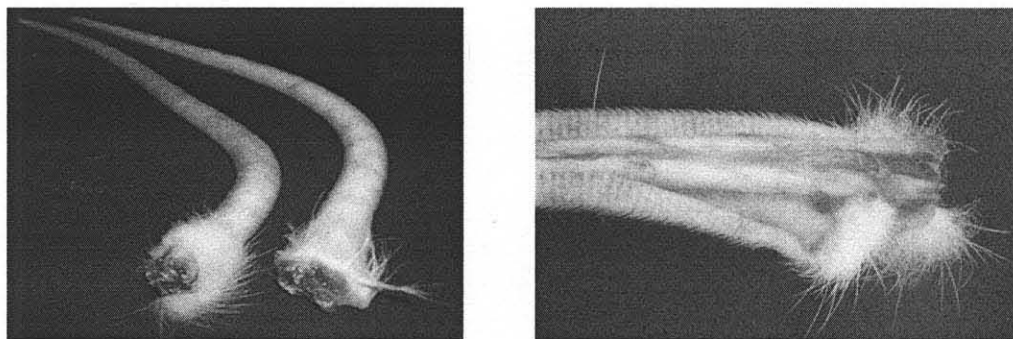
Figure 3.1 Rat tail dissection

Approximately 1-1.5 cm of the tail was picked up from the small end with a hemostat. The outer skin and hair dander was scrapped away using a scalpel 1-2 mm distal to the point from where the hemostat is applied. Then, bone-cutting forceps were used to fracture the vertebrate from the tip by rocking back and forth against the hemostat positioned on the proximal end of the tail. The cracked vertebrate fragments were slowly pulled away to separate from the rest of the tail. The attached tendons were also pulled out along with the detached vertebrate fragments and allowed to hang freely. The free hanging tendons were cut with scissors and placed in a pre-weighed dish of 50 ml sterile distilled water. Then, the hemostat was repositioned 1.5 cm toward the larger end of the tail and the procedure was repeated until all tendons were extracted from the entire length of the tail. Once all tendons were collected into the pre-weighed dish of water, the tendons combined with the pre-weighed 50 ml water was weighed and then subtracted

from the mass of the water to obtain the total mass of tendons. The tendons were extracted by immersing into 0.1% acetic acid sterile aqueous solution at (150 mL/1g tendon) for 5-7 days at 4°C with daily agitation (magnetic stir bar) for proper mixing to ensure efficient collagen extraction from tendons.

The mixture was decanted by slowly pouring the liquid phase into 50 mL polycarbonate centrifuge tubes without taking up the tendons and bulk matter. The raw collagen mixture was centrifuged at 3500 RPM for 30 minutes, keeping the supernatant (collagen), while the rest was discarded. The supernatant collagen solution was re-centrifuged at 2500 RPM for 10-15 minutes, and then the supernatant phase was collected once again while the solid pellet at the bottom was discarded.

The extracted collagen solution was transferred to dialysis tubing bags (MWCO 12,000-14,000) with lengths of 8-9 inches. The collagen extract solution was then dialyzed overnight at 4°C in pre-made dialysis buffer (Na_2HPO_4, NaH_2PO_4, pH 7.4). The resulting semi-solid gel collagen extract was transferred from dialysis tubing into 50 ml centrifuge tubes and spun at 3500 RPM for 30 min. The supernatant was discarded while retaining the collagen pellet for further processing. The tubes containing collagen were filled with 10-15 ml of 70% ethanol and spun at 1500 RPM for 10-15 min. The ethanol supernatant was decanted to obtain a sterile collagen semi-solid pellet at the bottom of the tube. The collagen semi-solid pellet can be stored up to several months at 4°C or indefinitely by freezing at -70°C.

The collagen end product following extraction and purification is a semi-solid gel containing excess moisture within the gel network. A dry weight form of the collagen end product is more desirable for preparing collagen dispersions with known

concentration by dry mass. Lyophilization, which is a freeze-drying technique, was used to obtain dry weight collagen from the semi-solid pellet form. The collagen semi-solid pellets were placed in an oven chamber under vacuum and dried by a high heat cycle including a freezing phase at -20°C. Rat tail collagen in lyophilized form exhibited a white porous sheet-like appearance. The dry weight lyophilized rat tail collagen was then dissolved in 0.02M acetic acid to obtain the desired collagen concentration (BD Biosciences, Product Sheet). In this study, dry weight lyophilized rat tail collagen was measured accordingly and dissolved in 0.02M acetic acid to yield a collagen concentration approximately 4.0 mg/ml.

3.2 Collagen Hydrogel Preparation

The neurite outgrowth response of fetal rat dorsal root ganglia (DRGs) in 3D hydrogel substrates in relation to varying rat tail collagen compositions was investigated. The 3D hydrogel was studied with particular interest since it closely mimics the natural 3D tissue architecture of neural tissue. The presence of type I collagen in nerve tissue make 3D collagen hydrogels a desirable component for nerve guide conduits.

The physiological environment significantly influences the physical properties of collagen. Collagen exists as a semi-solid gel at physiological pH and temperature (7.4 and 37°C), respectively. Therefore, these known properties of collagen can be used to create hydrogels *in vitro*. The stability of a hydrogel is dependent on maintaining both physiological pH and temperature. A series of pH buffers such as 10X MEM (Sigma M0275), HEPES, sodium bicarbonate ($NaHCO_3$) are required to sustain the physiological pH of 7.4 in a collagen hydrogel.

The preparation of a collagen 3D hydrogel involves mixing 10X MEM, HEPES, NaHCO₃, cell culture reverse osmosis water, 1.0M NaOH, and extracted rat tail collagen stock solution (~4.0 mg/ml). A stock solution of 10X MEM buffer solution was first prepared by adding HEPES and NaHCO₃ to 10X MEM using the following formulation:

Desired volume of 10X MEM + 59.58 g/L HEPES +22.0 g/L NaHCO₃

For 100 ml stock solution of 10X MEM: 5.98 g HEPES, 2.20 g NaHCO₃

In this case, 100 ml of 10X MEM was measured and added to a cold centrifuge tube followed by the addition of HEPES and NaHCO₃.

The 10X MEM stock solution, cell culture reverse osmosis water, 1.0M NaOH, and extracted rat tail collagen solution (~4.0 mg/ml) was mixed while working quickly on ice to prevent sudden gelling of collagen. For 3D cell culturing of DRGs, 3.2, 2.0, 0.8, and 0.6 mg/ml collagen gel concentrations were prepared. For 1 ml of gel, the ingredients mentioned above were mixed on ice at specific measured volumes based on desired collagen concentration (Table 3.1). For making collagen gel volumes other than 1 ml, the formulations were multiplied by the same factor to yield the desired overall volume of gel.

Table 3.1 Type I Collagen Hydrogel Formulations (total volume: 1 ml)

Collagen Hydrogels	3.2 mg/ml	2.0 mg/ml	0.8 mg/ml	0.6 mg/ml
10X MEM	100 µl	100 µl	100 µl	100 µl
Cell culture RO H₂O	88 µl	392 µl	697 µl	749 µl
1.0M NaOH	22 µl	20 µl	3 µl	1 µl
~4 mg/ml RT Collagen	800 µl	500 µl	200 µl	150 µl

3.3 Dorsal Root Ganglia Isolation

Tissue isolation of dorsal root ganglia (DRG) was performed at the Rutgers-Newark University Animal Facility. This protocol required the use of pregnant female rats ranging in 3-5 months of age. The pregnant female rat at E15 (day 15 following mating) was exposed with 100% CO_2 for 2-5 minutes (until rat ceases breathing for 30 seconds). If day 1 is considered the day after mating instead of day 0, then an E16 pregnant rat would also be acceptable. Furthermore, rat pups from an E16 pregnant rat have more firm spinal cords enabling an optimal yield of DRGs compared to premature or late stage rat pups.

The rat was placed on its back and the abdomen was sterilized with 70% ethanol. An incision was made from the tail to the thorax using scissors and forceps. In order to ensure death again, a thoractomy was performed by puncturing the diaphragm with scissors. A clean set of scissors and forceps were then used to perform a C-section by dissecting out the uterus and placing in a sterile 100 mm dish. The embryos were removed from the uterus while working under the dissection hood. The embryos were placed in Lebovitz L-15 or other non-CO_2 sensitive balanced medium.

Once the placenta membrane lining was removed from the embryos, the heads were cut off the embryos between the skull and the first vertebra. Micro-scissors or a micro knife was used to cut on the caudal side of the pronounced bump on the back of the head located under the ear and under the snout. The purpose of this step was to ensure that some of the brain stem is left over to handle for pulling out the cord. The anterior portion of the abdomen and limbs were then removed with the embryo on its side using the micro knife. The embryo was placed on its back, and the remaining viscera were removed with

fine forceps (Dumont #5) until there is a clear view of the vertebral column. A set of fine forceps (Dumont #5) was used to pinch through the vertebral column beginning at the rostal end. The brainstem and ménages were grasped with a #4-45 forceps and pulled straight up. Once taken out, the brainstem and ménages were placed in a 60mm dish with L-15 balanced medium. A fresh pair of Dumont #5 biologine-tip forceps was used to pluck off the DRGs from the isolated spinal cords. The DRGs were then placed in a 1.5 mL centrifuge tube with L-15 medium to be prepared for cell plating.

3.4 Cell Culturing of Dorsal Root Ganglia on 2D Collagen Substrates

The neurite outgrowth potential of fetal DRG explants on 2D plates coated with extracted type I rat tail collagen and type I bovine tendon collagen was analyzed in this study. A set of 35 mm Petri dishes was coated with 10 µg/ml of poly-L-lysine (PLL) as a base substrate for adhesion of DRG explants onto plastic dishes. Aliquots containing 1 ml of pre-made 1 mg/ml PLL were used to prepare a PLL concentration of 10 µg/ml. Therefore, 10 µg/ml PLL was made by adding 25 ml of sterile distilled water to 250 µl of PLL. The dishes were allowed to sit for a minimum of 1 hr to ensure PLL adsorbs onto the bottom surface of the plastic. Once a thin layer of PLL had adsorbed onto the surface, the PLL solution was removed, and the dishes were allowed to air-dry for 1 hr inside the tissue culture hood. Then, the dishes were rinsed three times (3x) with sterile cell culture water. The dishes were once again air-dried in the hood for a minimum of 1 hr prior to collagen coating. Once dried, a set of dishes can be prepared in advance and stored at $4^{\circ}C$ for up to two weeks. An ammonium hydroxide (NH_4OH) chamber was constructed using a 100x10 mm dish with the lid taped to a filter paper soaked in 1 mL

NH$_4$OH. Then, approximately 25-50 μL of extracted type I collagen from rat tail and bovine were applied and spread onto the surface of previously coated PLL dishes. The ammonium hydroxide vapors induced gelling of the collagen layer within 2-3 minutes. DRG explants were plated as 4 explants evenly spaced in the middle of the dish as 5 μL droplets. The DRGs were given 2 hours for adhesion onto the dishes. Once time was given for adhesion, approximately 2 ml of neuralbasal growth media was added. The neuralbasal growth media was made prior to DRG isolation by mixing 98 ml of Neuralbasal medium with B-27 and 0.4-0.5 mM L-Glutamine, 1 ml of 1% FBS heat inactivated, 1ml of 20% Glucose Sigma (25g in 100 ml water), and 1 μg of 10 ng/ml NGF (Gibco 13290-010) to make an approximately 100 ml stock solution of DRG neuralbasal growth media. The media in the dishes were changed every 2 days and the images were taken at day 1, 5, and 9 for axonal growth studies on the 2D substrates. The samples were viewed using a Nikon inverting microscope equipped with phase-contrast optics, fluorescent illumination, selective filters, and a digital image capture system. The images were later imported into Image J software program for performing neurite outgrowth measurements on each of the 2D substrates at day 1, 5, and 9. For each DRG isolation experiment, a set of 3 dishes (n = 3) was prepared for each collagen source: rat tail (extracted), bovine tendon (extracted), and commercial (BD Biosciences). The analysis of neurite outgrowth on 2D substrates was performed twice (n = 6) for each group of collagen substrates. DRGs were visualized using the Vybrant CFDA SE Cell Tracer Kit (Molecular Probes, Invitrogen).

3.5 Cell Culturing of Dorsal Root Ganglia on 3D Collagen Hydrogels

Dorsal root ganglia (DRG) neurite outgrowth in a hydrogel is a desirable approach since neural tissue is naturally grown in a 3D *in vivo* environment. Fetal DRG explants were plated within 3D type I collagen hydrogels of varying collagen concentrations (0.6, 0.8, 2.0, and 3.2 mg/mL) to study their neurite outgrowth. In a 24-well plate, a DRG explant was plated such that it is sandwiched between two collagen hydrogel layers. A DRG explant was plated on the bottom gel layer as a 10 µl drop and allowed 2 hours for adhesion to the surface. Then, the top gel layer was applied to embed the DRG explant within the two layers. The bottom layer was approximately 300 µm while the second top layer was roughly 100-150 µm thick. Once the top gel layer had solidified, approximately 2 ml of neuralbasal growth media, which was prepared with NGF and mitotic inhibitors as mentioned earlier, were added to the surface of the gel. In this case, minimizing the thickness of the overall hydrogel was important to enable diffusion of nutrients down to the DRG explants embedded within the gel.

The media in the wells were changed every 2 days and the images were taken at day 1, 5, and 9 for axonal growth studies within the 3D hydrogels. The samples were viewed using a Nikon inverting microscope equipped with phase-contrast optics, fluorescent illumination, selective filters, and a digital image capture system. The images were then imported into Image J software program for performing neurite outgrowth measurements on each of the 3D hydrogels at day 1, 5, and 9. A DRG isolation was often followed by a set of experiments consisting of two 24-well plates with two rows of

(n = 12) wells for each collagen gel concentration. This set of experiments was repeated twice for extracted rat tail type I collagen. The analysis of neurite outgrowth on 3D hydrogels was performed in triplicate (n = 9) for each collagen gel concentration.

3.6 Total Protein Assay for Type I Collagen Quantification

The validity of the type I collagen extraction process was assessed by quantifying protein concentration. There are several approaches to determine protein concentration including total protein assay. In this study, bicinchoninic acid (BCA) protein assay was the method of choice for assessing type I collagen concentration. The BCA protein assay (Pierce Biotechnology) is a colorimetric detection and quantification of total protein based on a bicinchoninic acid, which is a detergent-compatible compound often used as a fluorescence probe for colorimetric detection. This method consists of a well-known reaction mechanism involving the reduction of Cu^{2+} to Cu^{1+} by protein in alkaline medium with the highly sensitive and selective colorimetric detection of Cu^{+1} using a unique reagent containing bichinchonic acid. The chelation of two molecules of BCA with a Cu^{+1} ion yields a purple-colored reaction product in this assay. The water-soluble complex formed from this reaction exhibits a strong absorbance at approximately 570 nm with a nearly linear behavior for increasing protein concentrations over a broad working range (0.02 – 2.00 mg/ml).

The colorimetric detection of protein is based on the macromolecular structure of protein such as the number of peptide bonds and the presence of particular amino acids (cysteine, tryptophan, and tyrosine). The presence of these amino acid residues in protein is often attributed to color formation with BCA. In this assay, protein concentrations

were determined and reported with reference to standards of common proteins such as bovine serum albumin (BSA). A series of dilutions of known concentration were prepared from BSA and assayed together with the protein unknowns before the concentration of each unknown is determined by extrapolation based on the standard curve.

A set of diluted bovine serum albumin (BSA) standards was prepared in several clean vials or micropipette tubes using the same diluents. A 1 ml ampule of 2.0 mg/ml albumin standard was adequate to prepare a set of diluted standards for the microplate procedure (Table 3.2).

Table 3.2: Dilution Scheme for BSA Standards Preparation (Microplate Set-up)

Vial	Volume of Diluent	Volume and Source of BSA	Final BSA Concentration
A	0	300 µl	2.0 mg/ml
B	125 µl	375 ml	1.5 mg/ml
C	325 µl	325 ml	1.0 mg/ml
D	175 µl	175 ml	0.750 mg/ml
E	325 µl	325 ml	0.500 mg/ml
F	325 ml	325 ml	0.250 mg/ml
G	325 ml	325 ml	0.125 mg/ml
H	400 ml	100 ml	0.025 mg/ml
I	400 ml	0	0 mg/ml = Blank

The BSA standards were made by adding phosphate buffer saline (PBS) to 2.0 mg/ml albumin standard and thoroughly mixing in the micropipette tubes using a vortex machine and microcentrifuge. Once prepared, the BSA standards can be stored at -20°C. The extracted rat tail type I collagen and commercial rat tail type I collagen (BD Biosciences) were diluted 10X and 20X in 0.02M acetic acid or PBS for total protein assay. The diluents 0.02M acetic acid and PBS were selected to investigate if colorimetric reaction of type I collagen was affected by using different diluents. In this protein assay, the working reagent (WR) consisting of BCA was prepared by mixing 50 parts of reagent A with 1 part of reagent B (50:1, reagent A:B).

A 96-well microplate was used to load the BSA standards and unknowns (Table 3.3). The unknowns in this protein assay were the following: extracted rat tail type I collagen, commercial rat tail type I collagen (BD Biosciences), 0.02M acetic acid (AA), and PBS at 10X and 20X dilutions. A 10X dilution of collagen was prepared by adding 135 ml of AA or PBS to 15 ml of extracted rat tail collagen or commercial rat tail collagen (BD Biosciences). The 20X dilution of collagen was made by adding 142.5 ml of AA or PBS to 7.5 ml of extracted rat tail type I collagen or commercial rat tail type I collagen (BD Biosciences). For the microplate procedure, only 200 ml of WR reagent was required for each sample. When reagent B was first added to reagent A, turbidity was quickly observed but later disappeared upon mixing to yield a clear, green WR. In this experimental set-up, 0.5 ml of reagent B was added to 25 ml of reagent A to make the WR. Once all the samples were prepared and loaded into the 96-well microplate, a microplate reader programmed with Soft Max Pro Software was used to measure absorbance values of the samples at 570 nm.

Table 3.3: BCA Protein Assay Experimental Set-up (96-well Microplate)

A mg/ml	Std01 2.0	Std02 1.5	Std03 1.0	Std04 0.75	Std05 0.5	Std06 0.25	Std07 0.125	Std08 0.025	Std09 0
B mg/ml	Std01 2.0	Std02 1.5	Std03 1.0	Std04 0.75	Std05 0.5	Std06 0.25	Std07 0.125	Std08 0.025	Std09 0
C mg/ml	Std01 2.0	Std02 1.5	Std03 1.0	Std04 0.75	Std05 0.5	Std06 0.25	Std07 0.125	Std08 0.025	Std09 0
D	RT (AA) 10x	RT (AA) 10x	RT (AA) 10x	RT (AA) 10x	BL	RT (PBS) 10x	RT (PBS) 10x	RT (PBS) 10x	RT (PBS) 10x
E	RT (AA) 20x	RT (AA) 20x	RT (AA) 20x	RT (AA) 20x	BL	RT (PBS) 20x	RT (PBS) 20x	RT (PBS) 20x	RT (PBS) 20x
F	AA	AA	AA	AA	BL	PBS	PBS	PBS	PBS
G	BD (AA) 10x	BD (AA) 10x	BD (AA) 10x	BD (AA) 10x	BL	BD (PBS) 10x	BD (PBS) 10x	BD (PBS) 10x	BD (PBS) 10x
H	BD (AA) 20x	BD (AA) 20x	BD (AA) 20x	BD (AA) 20x	BL	BD (PBS) 20x	BD (PBS) 20x	BD (PBS) 20x	BD (PBS) 20x

*Std: BSA standards, RT: extracted rat tail type I collagen, BD: extracted bovine tendon type I collagen, AA: 0.02M acetic acid, PBS: Phosphate Buffer Saline

3.7 SDS-Polyacrylamide Gel Electrophoresis (PAGE)

Electrophoresis is a process in which charged molecules are transported through a solvent by an electrical field. This technique is a very simple, rapid, and sensitive analytical tool for separating proteins and nucleic acids. Any ion or molecule that carries a charge will migrate when placed in an electric field. Most biological molecules carry a net charge at any pH besides their isoelectric point and tend to migrate in relation to their charge density. When exposed to an electric field, the mobility of a biological molecule such as a protein is dependent on many factors including field strength, net charge on the molecule, size and shape of the molecule, and ionic strength and properties of the medium through which the molecules migrate.

Agarose and polyacrylamide gels are two types of support matrices used in electrophoresis. A support matrix serves as a porous media and behaves like a molecular sieve for migrating ions and molecules. The molecular sieving function of the matrix depends on the gel pore size of the matrix. Agarose, which has a large pore size, is ideal for separating macromolecules such as nucleic acids and protein complexes. Polyacrylamide has a smaller pore size and is more suitable for separating most proteins and smaller nucleic acids. In this study, polyacrylamide gels were used to run electrophoresis in order to investigate the purity of extracted rat tail type I collagen in comparison to the control commercial rat tail type I collagen (BD Biosciences).

Polyacrylamide gels are generated by the polymerization of acrylamide monomers into long chains and the cross-linking of these long chains by bifunctional compounds such as N,N-methylene-bisacrylamide at certain concentration of total monomer (%T) and proportion of cross linker (%C). If the acrylamide monomer

concentration (%T) is high, the overall pore size of the gel is quite small. A gel with a smaller pore size results in better resolution of low molecular weight molecules. Therefore, large molecules resolve well on low percentage gels while small molecules are best resolved on high percentage gels. The percentage gel is usually selected based on the size of the molecule being investigated.

Electrophoresis can be performed under denaturing conditions by using an anionic detergent such as sodium dodecylsulfate (SDS), which denatures and unfolds the proteins by wrapping around the hydrophobic portions of the protein. The resulting SDS-protein complexes are highly negatively charged and migrate through the gel based on their size rather than charge. Buffer systems are another essential component of electrophoresis and can be either continuous or discontinuous. A continuous buffer system uses only one buffer in the gel and the running buffer. In contrast, a discontinuous buffer system involves a different gel buffer and running buffer. Furthermore, a discontinuous buffer system consists of using at least two gel layers of different pore sizes, the stacking and resolving gel. The benefits to using a discontinuous buffer system are the concentration of the sample and higher resolution. In this study, SDS-PAGE was performed using a discontinuous buffer system using a running buffer different from the two gel buffers used to make the stacking and resolving gels.

The implementation of SDS-PAGE involved the preparation of several stock solutions and buffers prior to running an experiment. Acrylamide/Bis (30% T, 2.67% C) was either used pre-made or prepared by dissolving 87.6 g of acrylamide and 2.4 g of N,N-bis-methylene-acrylamide in 300 ml of nanopure water. Once prepared, the acrylamide/bis solution was stored at 4°C in the dark for up to 30 days. Then, 10% (w/v)

SDS was either used pre-made or prepared by dissolving 10 g of SDS in 90 ml of

nanopure water while gently stirring and bringing the total volume up to 100 ml with

water. Buffers for the resolving gel and stacking gel were prepared in stock by making

1.5M Tris-HCl, pH 8.8 (resolving gel) and 0.5M Tris-HCl, pH 6.8 (stacking gel). The

1.5M Tris-HCl buffer was prepared by adding 27.23 g of Tris base to 80 ml of nanopure

water while adjusting to pH 8.8 by adding 6N HCl. The total volume was then brought

up to 150 ml with nanopure water, and the solution was then stored at $4^{\circ}C$. The 0.5M

Tris-HCl buffer was prepared by adding 6.0 g of Tris base to 60 ml of nanopure water

while adjusting to pH 6.8 by adding 6N HCl. The total volume was then brought up to

100 ml with nanopure water, and the solution was then stored at $4^{\circ}C$. The sample buffer

(SDS reducing buffer) was used pre-made or prepared by mixing 3.55 ml of nanopure

water, 1.25 ml of 0.5M Tris-HCl, 2.5 ml of glycerol, 2.0 ml of 10% (w/v) SDS, and 0.2

ml of 0.5% (w/v) bromophenol blue to yield a total volume of 9.5 ml. The sample buffer

was then stored at room temperature until needed. The 10X electrode (Running) buffer,

pH 8.3 was also used pre-made or prepared by dissolving 30.3 g of Tris base, 144.0 g of

Glycine, and 10.0 g of SDS in nanopure water. The total volume was brought up to 1 L

with nanopure water. The 10X running buffer was then stored at $4^{\circ}C$ until further needed

for the experiment. The polymerizing agent ammonium persulfate (APS) was prepared

fresh on the day of the experiment. The 10% APS was made by dissolving 100 mg of

APS in 1 ml of nanopure water.

A 7% polyacrylamide gel was prepared by making the monomer solution by

adding the following ingredients: 5.1 ml of nanopure water, 2.3 ml of 30% degassed

acrylamide/bis, 2.5 ml of gel buffer (resolving gel buffer or stacking gel buffer), and 0.1

ml of 10% (w/v) SDS. For preparing the resolving gel, 50 μl of 10% APS and 5 μl of TEMED were added to the monomer solution and polymerization was initiated by gently swirling the solution. The stacking gel was made by adding 50 μl of 10% APS and 10 μl of TEMED to the monomer solution while initiating polymerization by gently swirling the solution.

The samples analyzed in SDS-PAGE were the extracted rat tail type I collagen and the commercial rat tail type I collagen (BD Biosciences). The maximum volume allowed for a 10 well comb of 1.0 mm thickness is 25 μl. Therefore, approximately 25 μl of each of the collagen samples were prepared by adding calculated volumes of sample buffer and 10X running buffer to each of the samples. Approximately 50 μl of B-Mercaptoethanol was added to 950 μl of pre-made sample buffer prior to adding to the samples. The samples were then heated in a water bath at 95oC for 4 min to initiate denaturation of collagen samples.

While the samples were in the water bath, the gels were casted by slowly pouring the resolving gel solution into the gel cassette. Once the resolving gel had solidified, the stacking gel solution was poured on top and allowed to solidify. A few drops of methanol were added to the very top of the casting gel to ensure a smooth surface on top of the gel during solidification. The 10-well comb was carefully inserted into the top of the gel to form the imprint wells for sample loading.

The gel solidified after 10 min and the 10-well comb was slowly taken out. Once the gel was placed into the XCell SureLock MiniCell electrophoresis chamber (Invitrogen Life Technologies), approximately 600 ml of 10X running buffer was poured into the upper chamber. While the gel was in the running buffer, the samples were then

loaded into the wells. A protein standard ladder was loaded into the first well and extracted rat tail and commercial rat tail collagen was loaded into the next two adjacent wells. The top of electrophoresis chamber was then connected to the anode and cathode ends of the core chamber. The ends of the electrode wires were connected to the positive and negative terminals of the Thermo EC Series 90 Power Supply (Thermo EC, Inc.) The power supply was programmed to a constant voltage of 125 V and a current range of 30-40 mA. Electrophoresis proceeded for approximately 90 min or until the bands run to the end of the gel. Once electrophoresis was completed, the power supple was turned off, electrodes disconnected, and the gel removed from the XCell SureLock MiniCell chamber. The gel then went through a series of staining in coomassie blue followed by several de-staining steps in order to visibly see the bands of the protein samples.

3.8 Wet Spinning of Type I Collagen

The 3D collagen hydrogel appears to be an essential supporting matrix for sustaining regenerating axons. However, additional components for facilitating guided axonal growth are most desirable for creating a nerve guide conduit. In this study, the aim was to fabricate sub-micron (2-10 μm) collagen fibers for use as a guiding component for DRG axonal outgrowth. The wet spinning technique was used to create collagen fibers from collagen dispersions of bovine type I collagen in 0.012N HCl. Collagen microfilament fibers were synthesized from 2% and 5% wt bovine collagen/0.012N HCl dispersions in ethanol. The protocol for making collagen monofilaments through the wet spinning process involves the following materials: collagen dispersions, acetone, ammonium hydroxide, and a pH meter.

An essential component of the wet spinning technique is the coagulation solution, which facilitates gelling of collagen dispersions. The coagulation solution was prepared by filling a container (glass or metal) with acetone. Ammonium hydroxide (NH_4OH) was added drop at a time into the acetone bath while the pH was monitored upon mixing the coagulation solution. The addition of ammonium hydroxide continued until the pH reached 9. The bovine collagen dispersions had a pH of approximately 4.5.

A syringe was filled with 5-10 ml of bovine collagen solution to be wet spun and the 17-gauge needle was secured to the syringe. The tip of the needle was slightly dipped into or just above the coagulation bath in order to extrude the collagen solution into the bath. The container used in this experimental set-up had a long and flat bottom. The tip of the syringe needle was moved from one end of the container to the other end as evenly as possible. This set-up seemed more desirable since a deep and narrow container would

only result in fibers that tend to tangle upon taking them out of the bath. The syringe was placed in a syringe pump and set to a flow rate of 10 ml/min. The extruded collagen dispersions coagulated into fibers within 5-10 min in the coagulation bath. The fibers were drawn out of the bath using a glass rod. The formed fibers were then hung on a "clothes line" to air dry to ensure efficient evaporation of solvent. During this initial stage of fiber development, the fibers were handled with delicate care since the fibers tend to break easily. Collagen dispersions from rat tail collagen yielded fibers that were too compliant. When wet-spun fibers from rat tail collagen were taken out of the bath to dry, they tended to break apart very easily. Therefore, collagen dispersions from bovine tendon were more favored for wet spinning collagen micro-fibers in this study. The fibers were allowed to air dry for 24 hr and then viewed at 4X magnification using a Nikon inverting microscope equipped with phase-contrast optics, fluorescent illumination, selective filters, and a digital image capture system. The images were later imported into Image J software program for characterizing fiber diameter of the wet spun collagen fibers. The protocol for wet spinning was repeated with an 18-gauge syringe needle to produce smaller collagen fibers at the same flow rate.

CHAPTER 4

RESULTS AND DISCUSSION

Fetal dorsal root ganglia (DRGs) were successfully cultured on both 2D collagen substrates and 3D collagen hydrogels. There was no inhibition of neurite growth during the 1, 5, and 9 day periods in duplicate studies for both 2D and 3D collagen substrates. A significant finding in this study showed that the DRGs grew just as well on extracted rat tail collagen as the commercial rat tail collagen from BD biosciences. Therefore, extracted rat tail collagen was conducive to DRG axon outgrowth. A comparison of neurite growth on 2D extracted rat tail and bovine tendon type I collagen surfaces revealed that bovine tendon collagen restricts DRG neurite extension. The axonal outgrowth response of DRGs in extracted 3D rat tail collagen hydrogels with varying collagen concentrations was expected. Collagen microfilaments were successfully wet spun from 2.0% and 5.0% wt extracted type I bovine tendon collagen dispersions in ethanol.

4.1 DRG Neurite Outgrowth on 2D Collagen Plates

The neurite outgrowth of dorsal root ganglia (DRGs) on 2D collagen dishes was imaged at 4X magnification using a Nikon inverting microscope equipped with phase-contrast optics, fluorescent illumination, selective filters, and a digital image capture system. The images were then imported into Image J software program for performing neurite outgrowth measurements. DRG neurite measurements were determined by dividing the DRG into top, bottom, left, and right quadrants. Five radial measurements were taken from each quadrant of the DRG neurites starting from the edge of the cell body to the tip

of the neurite. An average was taken of the five measurements from each quadrant and then a total average was further calculated from the four quadrants to determine the overall DRG neurite outgrowth. Some plates were stained with Vybrant to aid in imaging and measurement of DRG neurites at discrete time points. DRGs plated on 2D type I collagen dishes exhibited a gradual increase in neurite growth when monitored at days 1, 5, and 9 (Figure 4.1 a-c). DRG neurites on 2D extracted rat tail collagen appeared more dense compared to neurites on 2D extracted bovine tendon collagen.

a)   b)   c)   d)
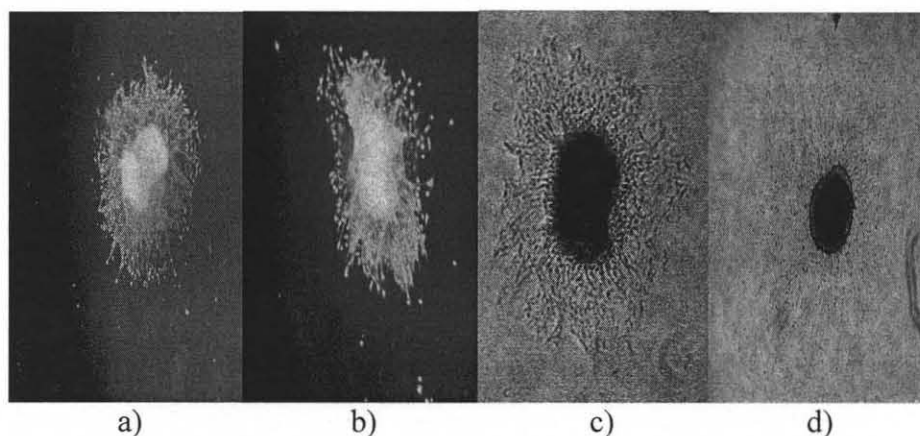
Figure 4.1 a) Extracted Type I Rat Tail Collagen Day 1 Vybrant stain, b) Extracted Type I Bovine Collagen Day 1 Vybrant Stain, c) Extracted Type I Rat Tail Collagen Day 5, d) Extracted Type I Bovine Collagen Day 5, 4X Magnification

DRG neurite outgrowth on 2D collagen substrates was studied in two separate experiments under the same conditions. DRGs exhibited a linear relationship in axonal outgrowth on 2D extracted rat tail collagen over the three discrete time points for both experiments. The second experiment revealed similar neurite outgrowth behavior over days 1, 5, and 9 and confirmed DRG neurite growth response on 2D extracted rat tail type I collagen coatings. An average of DRG neurite outgrowth measurements (n=6) for each

day was calculated using both experiments. Standard deviation of neurite outgrowth measurements was determined for each day. The highest deviation was seen in DRG neurite outgrowth at day 9 (Figure 4.2).

Figure 4.2 Plot of Mean DRG Axonal Growth at Days 1, 5, and 9 on 2D Extracted Rat Tail Type I Collagen Plates

The standard deviation for days 1, 5, and 9 was 8.89, 23.24, and 51.37, respectively. The neurite outgrowth on 2D extracted rat tail collagen increased from 32.4 μm up to an average of 272.6 μm by 9 days. The neurites appeared to be numerous and extended with ease on 2D extracted rat tail collagen.

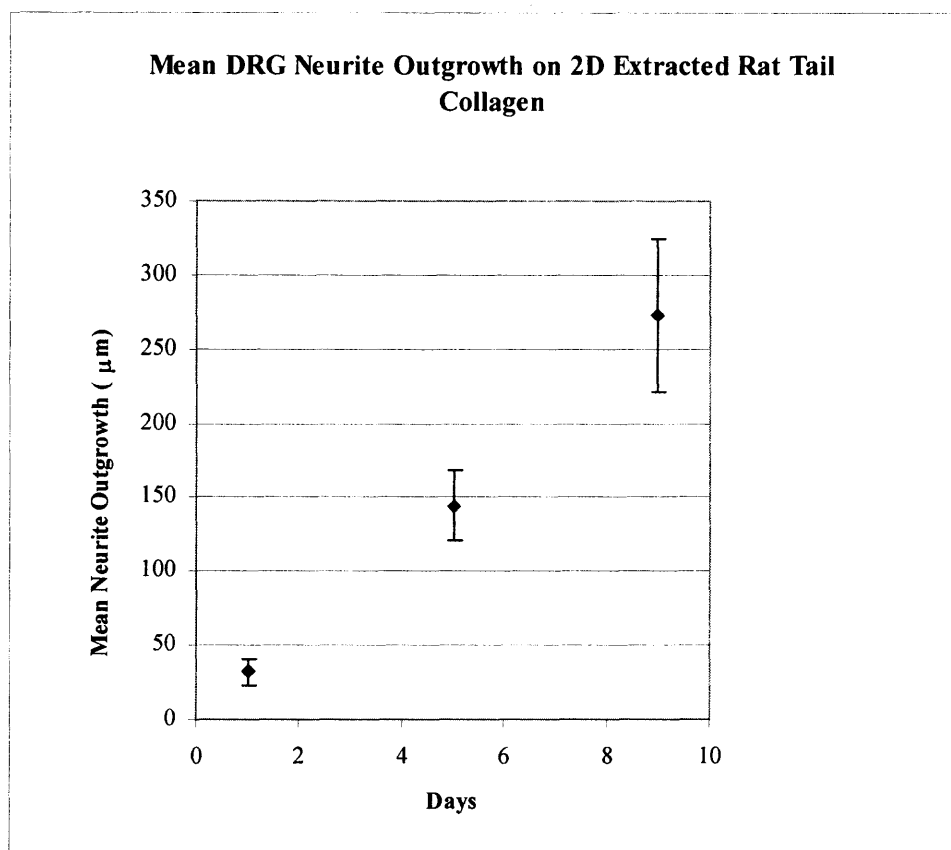The growth response of DRG neurites on extracted type I bovine tendon collagen was a linear relationship, but neurite extension appeared more limited over 9 days. In the first experiment, DRG neurites were limited to approximately 13 μm after day 1. The number of the neurites seemed less dense on bovine collagen compared to rat tail collagen. This observation may be due to the higher mechanical properties of bovine collagen, leading to a slight impedance of neurite outgrowth. The DRGs still appeared viable as their neurites continued extending over 9 days despite the mechanical constriction of bovine collagen. A second study of DRG neurite growth response on 2D bovine collagen surfaces conducted under the same conditions revealed similar neurite outgrowth behavior over days 1, 5, and 9 and confirmed DRG neurite growth response on 2D extracted bovine tendon type I collagen coatings. An average of DRG neurite outgrowth measurements (n=6) on 2D bovine tendon collagen dishes for each day was calculated using both experiments (Figure 4.3). Standard deviation of neurite outgrowth measurements on 2D bovine collagen surfaces was determined for each day. The highest deviation in DRG axonal growth on 2D bovine collagen was observed at day 9. The standard deviation for days 1, 5, and 9 was 9.31, 18.76, and 21.67, respectively. The neurite outgrowth on 2D extracted bovine tendon collagen increased from 14.8 μm up to an average of 156.8 μm by 9 days. The morphology and number of neurites on 2D bovine collagen had notable differences compared to rat tail collagen. The neurites seemed more sparse and restricted in extension on bovine collagen coated dishes.
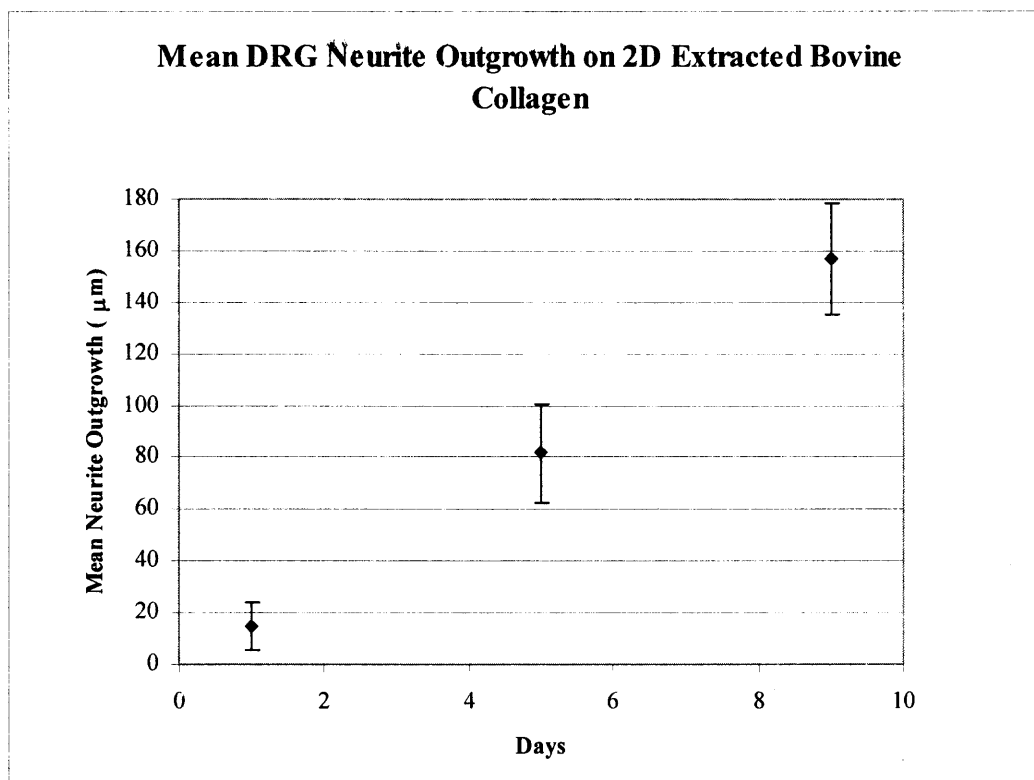
Figure 4.3 Plot of Mean DRG Axonal Growth at Days 1, 5, and 9 on 2D Bovine Tendon Type I Collagen Plates

A study of DRG neurite outgrowth was also conducted using commercial rat tail type I collagen (BD Biosciences). Axonal growth was investigated on commercial rat tail type I collagen at two separate experiments under the same conditions. Commercial rat tail type I collagen served as a comparison study with the extracted rat tail type I collagen. DRGs also exhibited a linear relationship in axonal outgrowth on 2D commercial rat tail collagen over the three discrete time points for both experiments. In the first experiment, DRGs grown on commercial rat tail type I collagen showed neurite growth up to approximately 298 μm after 9 days. The second study revealed a similar DRG neurite growth response on the 2D commercial rat tail type I collagen coatings.

The average of axonal growth measurements (n=6) from the two experiments were calculated and plotted along with standard deviations for each day (Figure 4.4).

Mean DRG Neurite Outgrowth on 2D Commercial Rat Tail Collagen
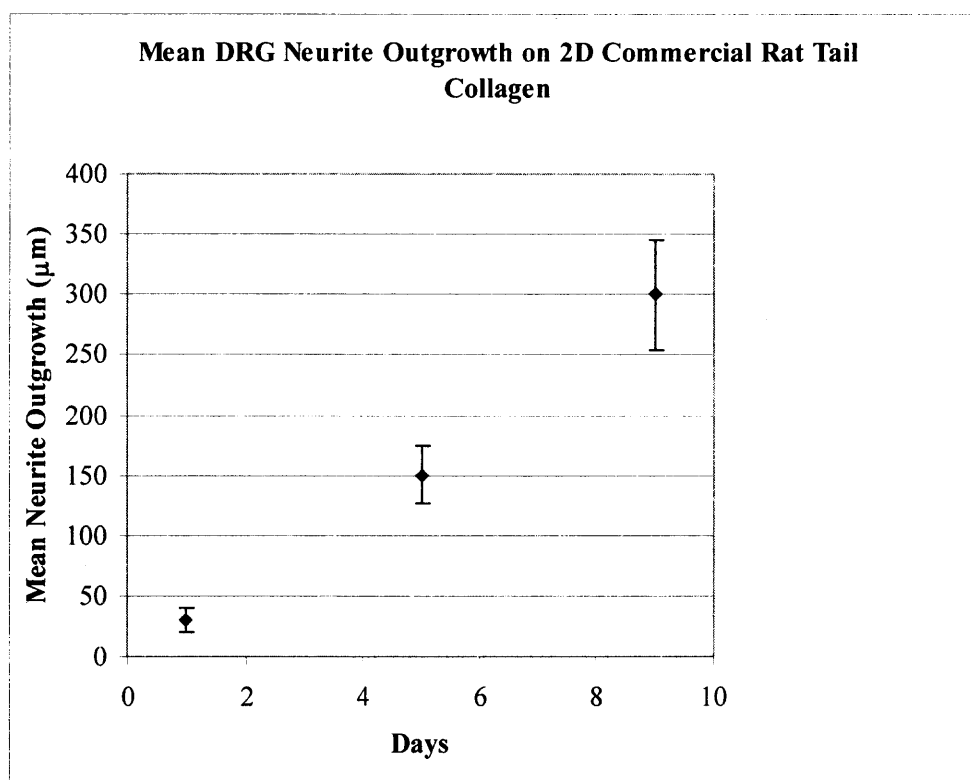
Figure 4.4 Plot of Mean DRG Axonal Growth at Days 1, 5, and 9 on 2D Commercial Rat Tail Type I Collagen Plates

Standard deviation of neurite outgrowth measurements on 2D commercial rat tail collagen surfaces for each day appeared similar to outgrowth studies on 2D extracted rat tail collagen. The highest deviation in DRG axonal growth on 2D commercial rat tail collagen was once again observed at day 9. The standard deviation for days 1, 5, and 9 was 9.66, 23.85, and 45.63, respectively. The neurite outgrowth on 2D commercial rat tail collagen increased from 30 μm up to an average of 299.6 μm by 9 days. The morphology and number of neurites on 2D commercial rat tail collagen revealed many

similarities to extracted rat tail collagen. The neurites were quite dense on the commercial rat tail collagen and exhibited optimal growth along the surface.

DRG neurite outgrowth over the three discrete time points exhibited a linear relationship for all 2D collagen substrates (Figure 4.5). Neurite outgrowth was most optimal after 9 days on commercial rat tail type I collagen (BD Biosciences). Extracted rat tail collagen closely matched the growth response of commercial rat tail collagen for days 1 and 5. Furthermore, the standard deviation of neurite outgrowth values for extracted rat tail collagen was similar to commercial rat tail collagen over 9 days. A comparison of 2D neurite outgrowth on all the 2D collagen substrates, once again revealed the limited axon growth on bovine collagen. A common finding in all 2D collagen substrates was the increase in standard deviation among the neurite outgrowth values from day 1 to day 9.
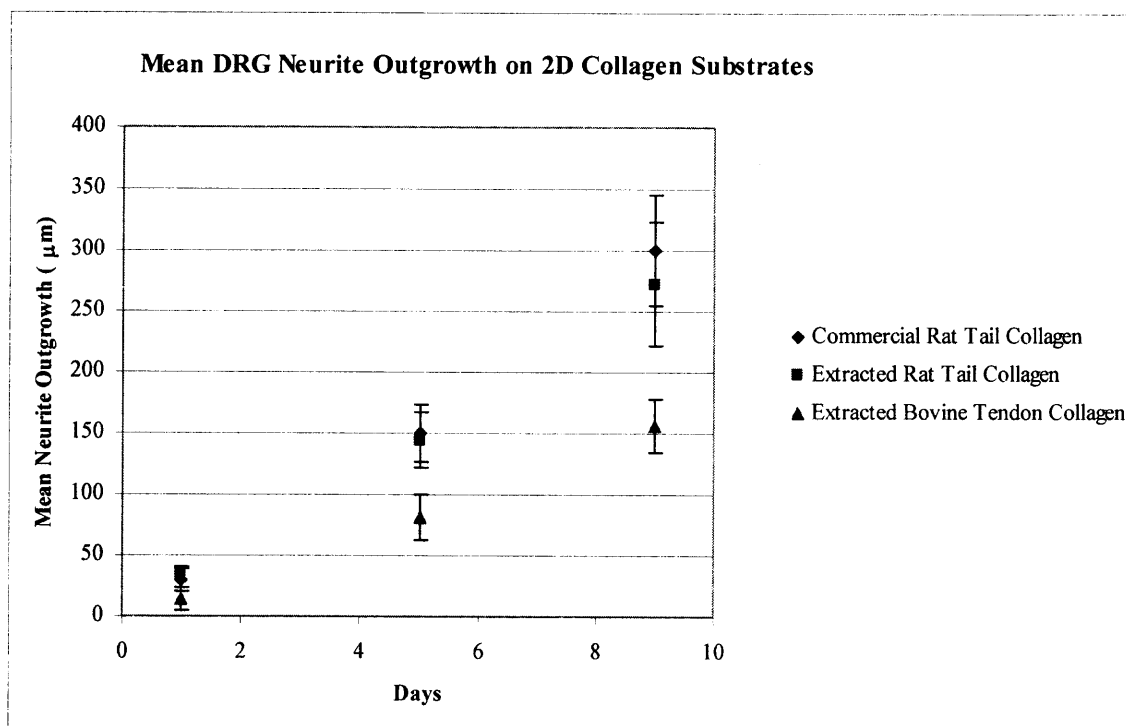
Figure 4.5 Comparison of Mean DRG Neurite Growth on all 2D Collagen Substrates

4.2 DRG Neurite Outgrowth on 3D Collagen Hydrogels

The neurite outgrowth of dorsal root ganglia (DRGs) on 3D collagen hydrogels was imaged at 4X magnification using a Nikon inverting microscope equipped with phase-contrast optics, fluorescent illumination, selective filters, and a digital image capture system. The images were then imported into Image J software program for performing neurite outgrowth measurements. DRG neurite measurements within 3D collagen hydrogels were taken similarly as with 2D collagen dishes by dividing the DRG into top, bottom, left, and right quadrants. Once again, five radial measurements were taken from each quadrant of the DRG neurites starting from the edge of the cell body to the tip of the neurite. An average was taken of the five measurements from each quadrant and then a total average was further calculated from the four quadrants to determine the overall DRG neurite outgrowth. For 3D neurite studies, the DRGs were embedded and grown inside collagen hydrogels contained within wells of a 24-well plate. Although some wells were stained with Vybrant to aid in imaging and measurement of DRG neurites, Vybrant staining within gels proved to be very difficult since the entire background was also stained along with the neurites. Therefore, image analysis and neurite measurements were performed using only phase-contrast images of the DRGs.

As expected, DRGs plated on 3D type I collagen gels also exhibited a gradual increase in neurite growth when monitored at days 1, 5, and 9. DRG axonal growth in 3D collagen hydrogels was repeated twice under the same conditions and collagen gel concentrations. The collagen gel concentration was directly related to the collagen gel

stiffness. Three-dimensional DRG axonal growth was later compared to two-dimensional outgrowth studies. In the first experiment, DRG neurites extended up to an average of 338 μm in length over 9 days in 0.8 mg/ml collagen gels. During days 1 and 5, DRG neurite outgrowth was highest for 0.6 mg/ml gels and gradually decreased in a nearly linear behavior with corresponding increase in collagen gel concentrations. By day 9, DRG neurite outgrowth was optimal in 0.8 mg/ml gels. The axonal growth response became more nonlinear over 9 days of cell culture.

The second experiment under the same conditions yielded a similar response in DRG neurite outgrowth over time. DRG neurites extended up to an average of 361 μm in length over 9 days in 0.8 mg/ml collagen gels. For the second experiment, DRG neurite outgrowth was once again highest for 0.6 mg/ml gels during days 1 and 5 and gradually decreased in a nearly linear behavior with corresponding increase in collagen gel concentrations. By day 9, DRG neurite outgrowth was optimal in 0.8 mg/ml gels. Neurite lengths were significantly lower for 2.0 and 3.2 mg/ml gel concentrations after day 9 in both experiments. The DRG neurite growth measurements were averaged between the two experiments and plotted along with standard deviation. Standard deviation in neurite outgrowth values was very small for day 1 but was more significant in days 5 and 9. DRG neurites grew up to an average of 349 μm by day 9 (Figure 4.5). Collagen gel concentration of 0.8 mg/ml appeared to be the most suitable matrix material for supporting DRG axonal growth over 9 days.
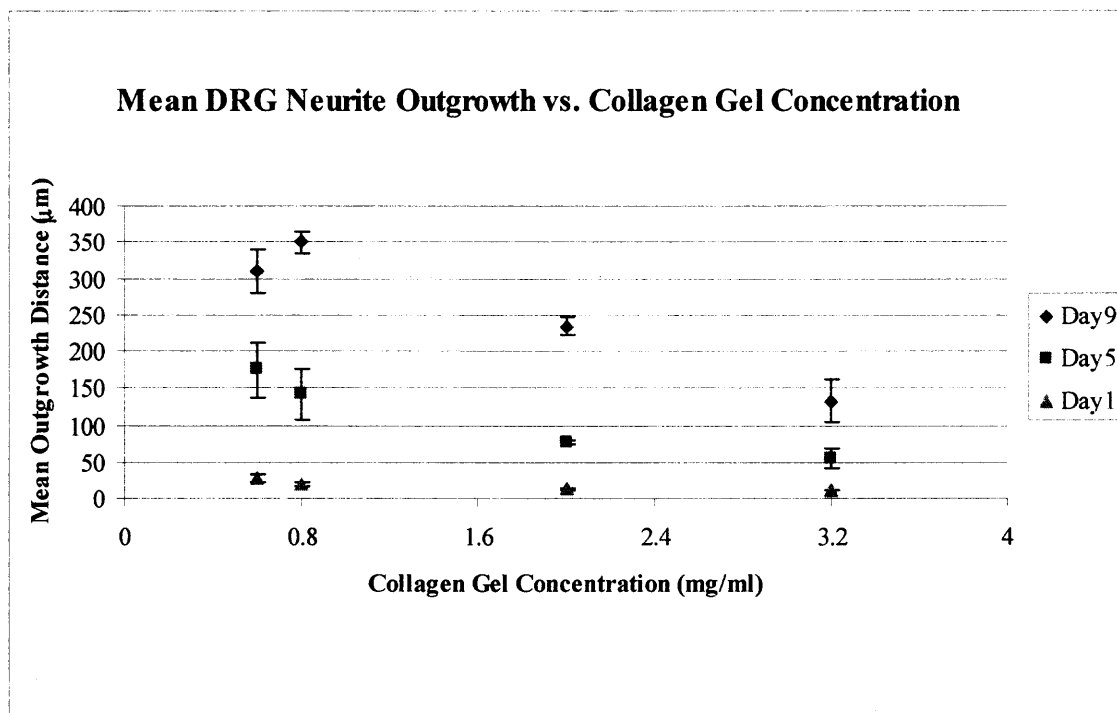
Figure 4.6 Plot of Mean DRG Axonal Growth at Days 1, 5, and 9 in 3D Extracted Rat Tail Collagen Hydrogels at 0.6, 0.8, 2.0, and 3.2 mg/ml collagen concentrations

A comparison of 2D and 3D DRG axonal outgrowth revealed that DRGs slightly favored the 3D environment over 9 days in cell culture (Figure 4.7). DRG neurite growth at day 1 was very close for both dimensions but performed better in 3D at days 5 and 9. The standard deviation in neurite outgrowth at day 9 in 3D was much lower than in 2D.
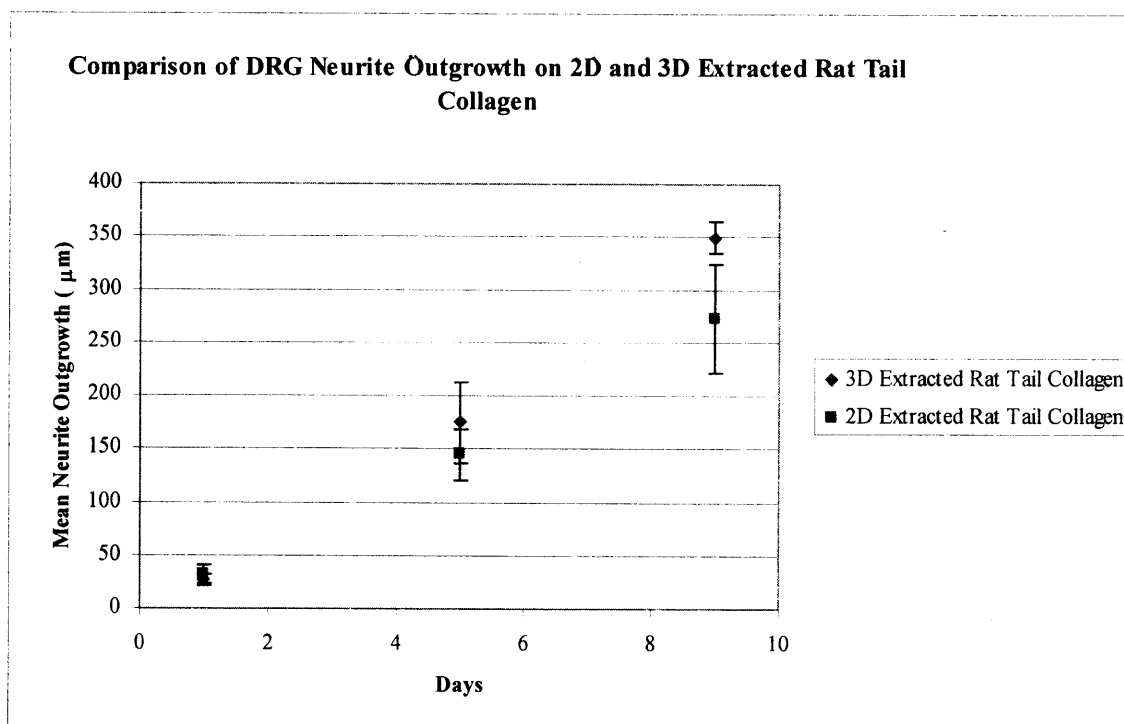
Figure 4.7 Plot of Mean DRG Axonal Growth at Days 1, 5, and 9 in 2D vs. 3D Extracted Rat Tail Collagen

4.3 Total Protein Assay for Type I Collagen Quantification

In total protein assay, extracted rat tail type I collagen and commercial rat tail type I collagen (BD Biosciences) were both quantified by colorimetric detection using the BCA reagent. PBS and 0.02M acetic acid were both used as diluents to determine which one would be more suitable for collagen detection in this assay. An analysis of the optical density values of both the extracted rat tail type I collagen and commercial rat tail type I collagen revealed high values when acetic acid was used as the diluent for both 10X and 20X dilutions (Table 4.1). Since collagen samples in PBS did not yield strong absorbance values, collagen unknowns in acetic acid were used to determine a rough estimate of collagen concentration. Acetic acid appeared to be a better diluent since the collagen was already in solution with 0.02M acetic acid for both the extracted and

commercial rat tail type I collagen. The average optical density for the extracted rat tail type I collagen in acetic acid was 0.18075 in 10X dilution. Furthermore, the average optical density for commercial rat tail type I collagen in acetic acid at 10X dilution was 0.1715. The average optical density for extracted rat tail collagen and commercial rat tail collagen in acetic acid at 20X dilution was 0.1123 and 0.0975, respectively. A best-fit linear regression line was made by plotting the optical density values and corresponding concentrations of the BSA standards (Figure 4.10). The equation $y = 1.0449x + 0.0706$ was determined from the best-fit line, where y is the optical density value and x represents concentration. The correlation of optical density to concentration for the BSA standards was 0.9899. The concentrations of the collagen unknowns were then calculated using the equation. The calculated concentration of extracted rat tail type I collagen and commercial rat tail type I collagen at 10X dilution was approximately 0.1054 and 0.09656 mg/ml, respectively. Furthermore, the concentration for extracted rat tail type I collagen and commercial rat tail type I collagen at 20X dilution was calculated to be approximately 0.03986 and 0.02574 mg/ml. The optical density and concentration values for both extracted rat tail type I collagen and commercial type I collagen for both dilutions closely matched each other indicating that the extracted rat tail type I collagen exhibited similar chemical properties to the commercial rat tail type I collagen based on absorbance values from the protein assay. BCA total protein assay was sufficient to confirm that there were similar chemical properties of extracted rat tail type I collagen to the control commercial rat tail type I collagen (BD Biosciences). However, other protein detection techniques may be more accurate and should be considered.

Table 4.1 Optical Density and Concentration Values of Collagen Unknowns in BCA Total Protein Assay

Unknowns RT	Samples; dilution:		10X
D	0.178	0.127	
	0.184	0.131	
	0.175	0.136	
	0.186	0.129	
Ave	0.18075	0.13075	
Concentration (mg/ml)	**0.105416786**	**0.057565317**	
Unknowns BD	Samples; dilution:		10X
G	0.162	0.075	
	0.165	0.083	
	0.179	0.097	
	0.18	0.085	
Ave	0.1715	0.085	
Concentration (mg/ml)	**0.096564265**	**0.013781223**	
Unknowns RT	Samples; dilution:		20X
E	0.108	0.076	
	0.112	0.077	
	0.111	0.073	
	0.118	0.077	
Ave	0.11225	0.07575	
Concentration (mg/ml)	**0.039860274**	**0.004928701**	
Unknowns BD	Samples; dilution:		20X
H	0.093	0.046	
	0.099	0.052	
	0.095	0.048	
	0.103	0.053	
Ave	0.0975	0.04975	
Concentration (mg/ml)	**0.02574409**	**-0.019954063**	

Concentration values of extracted rat tail collagen and commercial rat tail collagen were much lower than the expected concentration (~4.0 mg/ml RT and 3.63 mg/ml BD). The concentration of the commercial rat tail collagen as highlighted by the circle on the standard curve was approximately 0.966 mg/ml (Figure 4.8). Furthermore, the concentration of the extracted rat tail collagen also highlighted on the graph was approximately 1.05 mg/ml.

BCA Protein Assay Standard Curve

$y = 1.0449x + 0.0706$
$R^2 = 0.9899$

Absorbance @ 570nm (O.D.)

Concentration (mg/mL)

Series1
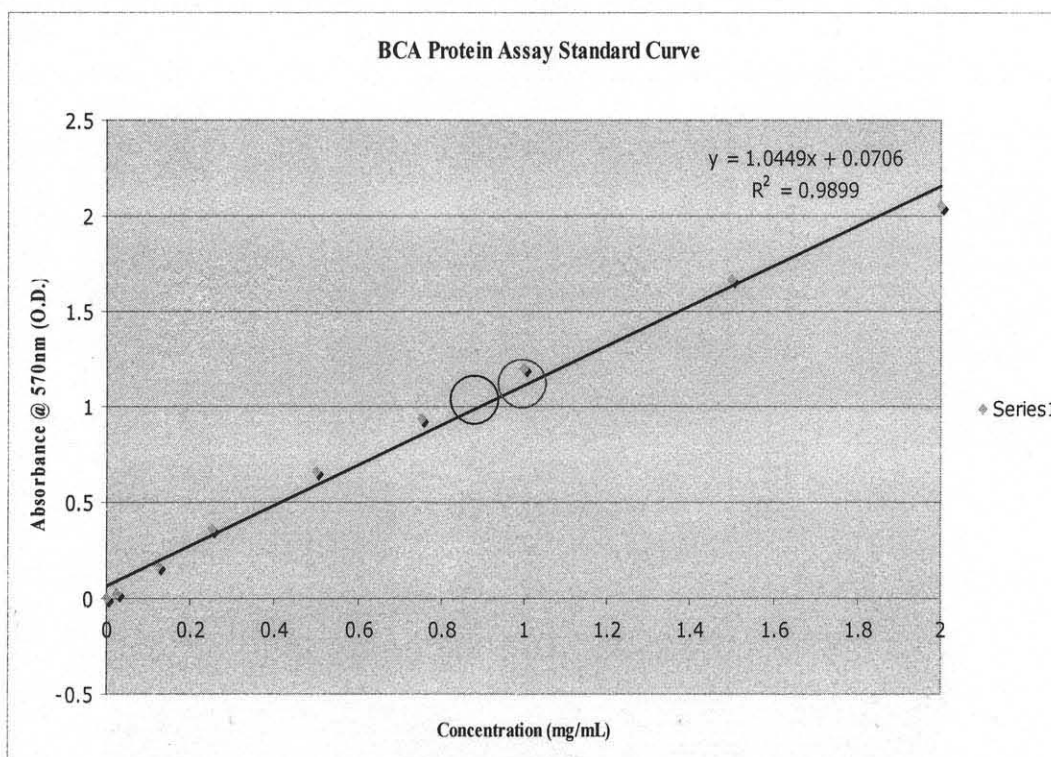
Figure 4.8 BCA Total Protein Assay (Standard Curve of BSA Standards)

4.4 SDS-Polyacrylamide Gel Electrophoresis (PAGE)

The results of SDS-PAGE revealed that the extracted rat tail type I collagen was

qualitatively similar to the commercial rat tail type I collagen based on the banding

patterns. Although the bands for the extracted rat tail type I collagen matched up well to

the bands for commercial rat tail collagen, only the bands for commercial rat tail collagen

were more visible. The protein standard ladder was used as a comparison to quantify the

protein bands of the sample unknowns. Doublet bands present at 235 kDa and 215 kDa

and another pair of doublets at 130 kDa and 115 kDa are characteristic of rat tail type I

collagen. These two doublet pairs were present in both commercial and extracted rat tail

collagen (Figure 4.9). However, the bands for the extracted collagen were very faint

suggesting that only small amounts of type I collagen was present following the

extraction process.
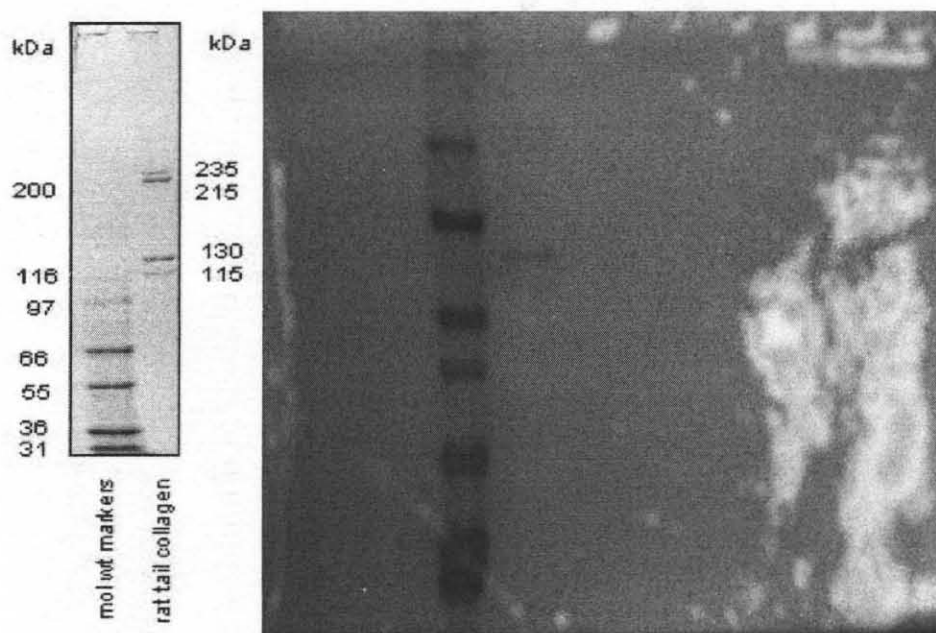
Figure 4.9 Protein bands of the protein ladder, commercial rat tail collagen, and extracted rat tail collagen (left to right)

4.5 Wet Spinning Results and Fiber Diameter Characterization

The wet spinning technique was used to synthesize collagen micron fibers using collagen dispersions of type I bovine collagen in 0.012N HCl. Bovine type I collagen/0.012N HCl was dissolved in 100% wt ethanol to create collagen dispersions for wet spinning fibers. In this study, 100% wt ethanol was selected as the solvent since it evaporates at a fast rate, which is ideal for solidification of wet-spun fibers following fiber extrusion in the coagulation bath. In this study, 2%, 5%, and 30% wt type I bovine collagen/0.012N HCl dispersions in ethanol were prepared for wet spinning collagen fibers. In this study, 17-gauge and 18-gauge syringe needles were selected for wet spinning collagen fibers. Extracted type I rat tail collagen was also wet-spun under the same weight percentages in ethanol but yielded only soft fibers which tended to break easily. Type I bovine collagen dispersions resulted in stronger wet-spun fibers. Wet-spun fibers synthesized from 30% wt bovine collagen produced very thick fibers with beading and rough non-uniform surfaces. The bovine collagen dispersions with 2% and 5% wt in ethanol at a flow rate of 10 ml/min yielded fibers with desirable fiber diameters (Figure 4.10).

a)   b)   c)   d)

Figure 4.10 a) 2% wt type I bovine collagen, 17G, b) 5% wt type I bovine collagen, 17G, c) 2% wt type I bovine collagen, 18G, d) 5% wt type I bovine collagen, 18G, 4X magnification

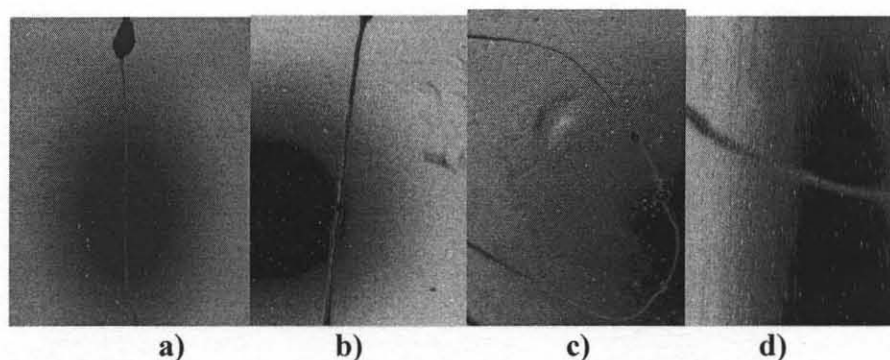Some images were taken at 4X magnification of wet-spun fibers produced from 2% and 5% wt bovine collagen dispersions using a Nikon inverting microscope. The images were imported into Image J software for fiber characterization of wet-spun fibers. The diameter of wet-spun fibers was determined by taking diameter measurements along the length of a fiber. Five measurements were taken at five discrete regions along the length of the fiber (n=25). Each of the five measurements at the different segments of the fiber was averaged and an overall total average was calculated. The average of measurements taken from two fibers wet-spun from 2% wt bovine collagen using a 17-gauge needle yielded a mean diameter of approximately 2.297 μm (Table 4.2).

A set of measurements was also taken of wet-spun fibers made from 5% wt bovine collagen using a 17-gauge needle. The mean diameter of 5% wt bovine collagen wet-spun fibers was approximately 2.536 μm (Table 4.3). The increase in weight percentage from 2% wt to 5% wt bovine collagen while using the same needle diameter and flow rate resulted in wet-spun fibers with increased fiber diameters. Therefore, the parameters established for wet spinning and the 17-gauge needle were suitable for attaining submicron collagen fibers.

Wet-spun fibers made from 2% and 5% wt bovine collagen using an 18-gauge needle were also measured. The mean diameter of 2% wt bovine collagen wet-spun fibers was approximately 1.389 μm (Table 4.4). Furthermore, the mean diameter of 5% wt bovine collagen fibers using an 18-gauge needle was 1.428 μm. Once again, the flow rate and the 18-gauge needle were ideal for obtaining sub-micron collagen fibers.

Table 4.2 2% wt Bovine Collagen Wet-spun Fibers, 17G Needle, (n=50)

Fiber 1: 2% wt 17G Needle			Fiber 2: 2% wt 17G Needle		
Measurements		Avg	Measurements		Avg
1	1.271	1.5382	1	2.292	2.4598
2	1.421		2	2.292	
3	1.348		3	2.734	
4	1.853		4	2.247	
5	1.798		5	2.734	
6	1.907	2.3168	6	2.247	2.5334
7	2.542		7	2.292	
8	2.01		8	2.697	
9	2.878		9	2.697	
10	2.247		10	2.734	
11	3.241	3.485	11	1.798	1.708
12	3.866		12	1.798	
13	3.623		13	1.348	
14	3.272		14	1.798	
15	3.423		15	1.798	
16	1.421	2.6242	16	1.798	1.6472
17	2.42		17	1.421	
18	2.842		18	1.421	
19	3.423		19	1.798	
20	3.015		20	1.798	
21	2.01	2.286	21	1.853	2.373
22	2.542		22	1.853	
23	2.01		23	2.247	
24	2.621		24	3.178	
25	2.247		25	2.734	
		Sub. Avg			Sub. Avg
		2.450 μm			**2.144 μm**
				Total	**2.297 μm**

Table 4.3 5% wt Bovine Collagen Wet-spun Fibers, 17G Needle, (n=25)

Fiber 3: 5% wt 17G Needle		
Measurements		Avg
1	2.842	2.626
2	2.420	
3	2.734	
4	2.292	
5	2.842	
6	2.734	2.7334
7	2.697	
8	2.697	
9	2.842	
10	2.697	
11	2.292	2.4434
12	2.247	
13	2.697	
14	2.247	
15	2.734	
16	2.292	2.801
17	2.247	
18	2.697	
19	3.146	
20	3.623	
21	1.798	2.0786
22	1.798	
23	1.853	
24	2.247	
25	2.697	
		Total Avg
		2.536 μm

Table 4.4 2% wt Bovine Collagen Wet-spun Fibers, 18G Needle, (n=25)

Fiber 4: 2% wt 18G Needle		
Measurements		Avg
1	1.421	1.2246
2	1.421	
3	1.005	
4	1.005	
5	1.271	
6	1.421	1.7004
7	1.62	
8	1.421	
9	1.62	
10	2.42	
11	1.421	1.2254
12	1.005	
13	1.005	
14	1.348	
15	1.348	
16	1.711	1.6
17	1.920	
18	1.439	
19	1.310	
20	1.620	
21	1.271	1.1946
22	1.005	
23	1.271	
24	1.421	
25	1.005	
		Total Avg
		1.389 μm

Table 4.5 5% wt Bovine Collagen Wet-spun Fibers, 18G Needle, (n=25)

Fiber 5: 5% wt 18G Needle		
Measurements		Avg
1	2.022	2.278
2	2.258	
3	2.346	
4	2.472	
5	2.292	
6	1.124	1.3964
7	1.348	
8	1.589	
9	1.348	
10	1.573	
11	1.573	1.4868
12	1.367	
13	1.348	
14	1.348	
15	1.798	
16	1.348	1.1686
17	1.348	
18	1.124	
19	1.124	
20	0.899	
21	0.674	0.809
22	0.674	
23	0.899	
24	1.124	
25	0.674	
		Total Avg
		1.428 μm

Table 4.6 Average Fiber Diameters for 2% and 5% wt Bovine Collagen Wet-spun Fibers

Average Fiber Diameters	17 G Needle	18 G Needle
2% wt bovine collagen	2.297 ± 0.436 µm	1.389 ± 0.212 µm
5% wt bovine collagen	2.536 ± 0.254 µm	1.428 ± 0.476 µm
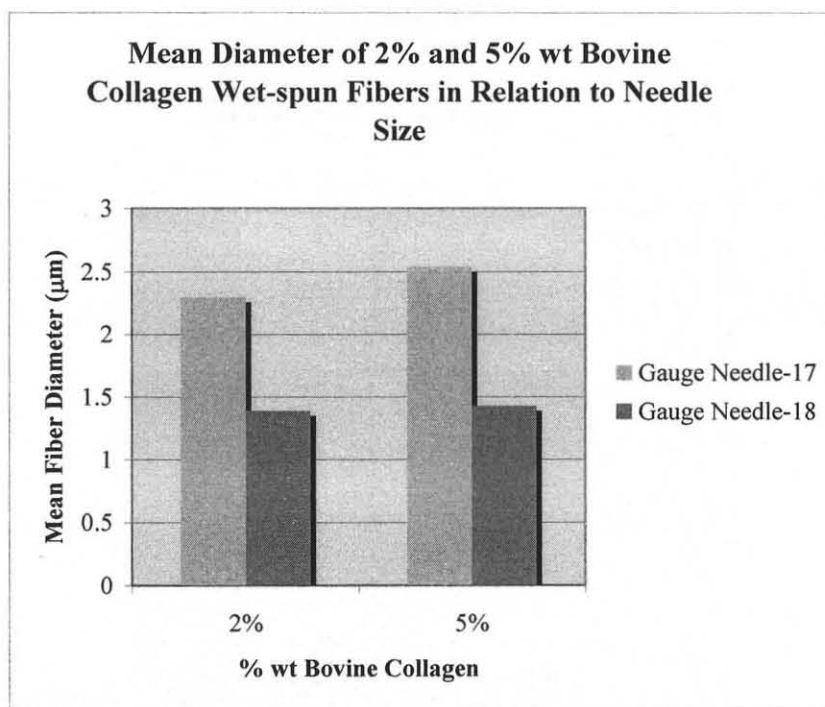
Figure 4.11 Mean Diameter of 2% and 5% wt Bovine Collagen Wet-Spun Fibers in Relation to Needle Gauge Size

CHAPTER 5

CONCLUSION AND FUTURE WORK

5.1 Summary of DRG Neurite Growth on 2D Collagen Dishes

DRG neurite outgrowth on 2D collagen substrates exhibited an overall linear relationship over days 1, 5, and 9. Neurite extension on 2D extracted rat tail collagen closely matched the results observed on 2D commercial rat tail collagen (BD Biosciences). Neurites appeared to be numerous and extended with ease on both 2D extracted rat tail and commercial rat tail collagen. The morphology and number of neurites on 2D bovine collagen had notable differences compared to rat tail collagen. The neurites seemed more sparse and restricted in extension on bovine collagen coated dishes. This observation may be due to the higher mechanical properties of bovine collagen, leading to a slight impedance of neurite outgrowth. The common observation among all 2D collagen substrates was the increase in standard deviation of neurite outgrowth values from day 1 to day 9. A comparison of growth studies on 2D collagen substrates revealed that axonal outgrowth was most optimal after 9 days on commercial rat tail type I collagen (BD Biosciences).

5.2 Summary of DRG Neurite Growth on 3D Collagen Hydrogels

Dorsal root ganglia (DRG) neurite outgrowth in a hydrogel is a desirable approach since neural tissue is naturally grown in a 3D *in vivo* environment. Fetal DRG explants plated within 3D type I collagen hydrogels of varying collagen concentrations (0.6, 0.8, 2.0, and 3.2 mg/ml) exhibited optimal neurite extension in 0.8 mg/ml gels after 9 days of cell culture. The sandwich method for embedding DRG explants between two hydrogel

layers proved successful, and the DRGs remained viable by day 9. Standard deviation in neurite outgrowth values was very small for day 1 but was more significant in days 5 and 9. DRG neurites grew up to an average of 349 μm by day 9, exceeding neurite outgrowth on 2D substrates. An average of DRG axonal growth between two experiments confirmed that a collagen gel concentration of 0.8 mg/ml appear to be the most suitable matrix material for supporting optimal DRG axonal growth over 9 days. Although the initial assumption was that DRG axonal growth would be more favored on 2D collagen substrates due to the presence of a rigid surface, the results were contradictory and indicated that further studies of two and three-dimensional axonal outgrowth on collagen should be conducted. Furthermore, image analysis of DRG neurites embedded in hydrogels stained with Vybrant proved to be difficult to visualize since the entire gel was also stained along with the neurites.

5.3 Summary of Total Protein Assay

The validity of the type I collagen extraction process was assessed by quantifying protein concentration using BCA total protein assay. Extracted rat tail type I collagen and commercial rat tail type I collagen (BD Biosciences) were both quantified by colorimetric detection using the BCA reagent. A comparison of collagen detection using two different diluents revealed that 0.02M acetic acid was the more appropriate diluent since the optical density values of both the extracted rat tail type I collagen and commercial rat tail type I collagen revealed high values when acetic acid was used as the diluent for both 10X and 20X dilutions. Acetic acid most likely yielded higher absorbance values since the collagen was already in solution with 0.02M acetic acid for both the extracted and commercial rat tail type I collagen. A best-fit linear regression line constructed from the

optical density values and corresponding concentrations of the BSA standards resulted in a correlation of 0.9899 between optical density values and the concentration of the BSA standards. The calculated concentration of extracted rat tail type I collagen and commercial rat tail type I collagen at 10X dilution was approximately 0.1054 and 0.09656 mg/ml, respectively. Therefore, the BCA total protein assay indicated that the concentration of extracted rat tail and commercial rat collagen was approximately 1.05 and 0.966 mg/ml, respectively. These values were significantly lower than the expected concentrations of extracted rat tail collagen (~4.0 mg/ml) and commercial rat tail collagen (3.63 mg/ml). Since the absorbance values for the collagen samples were very low, the results of BCA total protein assay were difficult to interpret for comparing extracted rat tail to commercial rat tail collagen. The low absorbance values for rat tail type I collagen in this assay were likely attributed to poor solubility of collagen at certain molecular weights. The absorbance values from BCA total protein assay more resembled a small fraction of collagen that was soluble in the diluent. Therefore, other analytical techniques that confront this solubility issue during collagen quantification are more desirable.

5.4 Summary of SDS-Polyacrylamide Gel Electrophoresis (PAGE)

Although SDS-PAGE revealed that the extracted rat tail type I collagen was qualitatively similar to the commercial rat tail type I collagen, the faint bands observed in the extracted rat tail collagen indicated a very low presence of type I collagen in the end-product of the extraction. Therefore, the collagen extraction and purification process needs to be further assessed to ensure that the end-product contains the same amount of type I collagen as the commercially extracted rat tail collagen from BD Biosciences. An analysis of the gel

showed doublet bands at 235 kDa and 215 kDa and another pair of doublets at 130 kDa and 115 kDa, indicating the presence of rat tail type I collagen in both the extracted and commercial rat tail collagen samples.

5.5 Summary of Wet Spinning Results

The wet spinning technique was used to create collagen micron fibers from collagen dispersions of bovine type I collagen in 0.012N HCl. Collagen microfilament fibers were successfully synthesized from 2% and 5% wt bovine collagen/0.012N HCl dispersions in ethanol. From the 2%, 5%, and 30% wt type I bovine collagen/0.012N HCl dispersions, the 2% and 5% wt bovine collagen dispersions yielded wet spun collagen fibers that met the sub-micron diameter range. The increase in weight percentage from 2% wt to 5% wt bovine collagen while using the same needle diameter and flow rate resulted in wet-spun fibers with increased fiber diameters. An increase in weight percentage of bovine collagen dispersions was directly related to the viscosity of the solution. An 18-gauge needle with a flow rate of 10 ml/min was used to produce collagen fibers as small as 1.398 µm in diameter. According to a previous study, DRGs exhibited optimal axonal outgrowth along polypropylene fibers as small as 5 µm [18]. Although the diameter range of wet-spun fibers was achieved in this study, the process must be further modified to yield more consistent diameters throughout the length of the fiber.

5.5 Future Work

The comparison of DRG axonal outgrowth studies on two and three-dimensional collagen substrates revealed that further studies are essential to understand the behavior of neurite extension on rigid and compliant materials. Although the hypothesis was that DRG axon growth on 2D surfaces would be more favored, the results of this study did not confirm the hypothesis. The results of wet spinning type I bovine collagen for creating collagen fibers in the micron scale looks promising. Furthermore, future studies will be conducted to functionally modify these wet-spun collagen fibers with biomolecules or neurotrophins to further enhance neurite sprouting and growth along fibers. The next phase of research is to study DRG axonal outgrowth along wet-spun fibers and compare their growth to previous studies of outgrowth on 2D and 3D collagen substrates. A better technique to visualize DRG neurites in 3D collagen hydrogels will be determined such as using confocal microscopy along with other staining cell markers or molecular probes such as calcein AM. This study revealed that BCA total protein assay was not an effective analytical tool for quantifying type I rat tail collagen. In future studies, other protein assays such as enzyme-linked immunosorbent assay (ELISA) will be considered as an alternate approach to quantifying collagen.

REFERENCES

1. Deumens, R., Koopmans, G. C., & Joosten, E. A. J. (2005). Regeneration of descending axon tracts after spinal cord injury. *Progress in Neurobiology, 77*(1-2), 57-89.

2. Iannotti, C., Li, H., Yan, P., Lu, X., Wirthlin, L., & Xu, X. (2003). Glial cell line-derived neurotrophic factor-enriched bridging transplants promote propriospinal axonal regeneration and enhance myelination after spinal cord injury. *Experimental Neurology, 183*(2), 379-393.

3. Jain, A., Kim, Y., McKeon, R. J., & Bellamkonda, R. V. (2006). In situ gelling hydrogels for conformal repair of spinal cord defects, and local delivery of BDNF after spinal cord injury. *Biomaterials, 27*(3), 497-504.

4. Schmidt, C.E. and Leach, J.B. (2003). Neural Tissue Engineering: Strategies for Repair and Regeneration. *Annu. Rev. Biomed. Eng. 5*, 293-347.

5. Pfister, B. J., Iwata, A., Taylor, A. G., Wolf, J. A., Meaney, D. F., & Smith, D. H. (2006). Development of transplantable nervous tissue constructs comprised of stretch-grown axons. *Journal of Neuroscience Methods, 153*(1), 95-103.

6. Piantino, J., Burdick, J. A., Goldberg, D., Langer, R., & Benowitz, L. I. (2006). An injectable, biodegradable hydrogel for trophic factor delivery enhances axonal rewiring and improves performance after spinal cord injury. *Experimental Neurology, 201*(2), 359-367.

7. Iwata, A. et al. (2006). Long-term survival and outgrowth of mechanically engineered nervous tissue constructs implanted into spinal cord lesions. *Tissue Engineering, 12*(1), 101-110.

8. Xu, X. et al. (2003). Peripheral nerve regeneration with sustained release of poly(phosphoester) microencapsulated nerve growth factor within nerve guide conduits. *Biomaterials, 24*, 2405-2412.

9. Willits, R. K. and Skornia, S.L. (2004). Effect of collagen gel stiffness on neurite extension. *J. Biomater. Sci. Polymer Edn, 15(12)*, 1521-1531.

10. Rizvi, A.H., Wasserman, A.J., Zazanis, G., Silver, F.H., (1991). Evaluation of peripheral nerve regeneration in the presence of longitudinally aligned collagen fibers. *Cell Mater, 1*, 279-289.

11. Yoshii, S., Oka, M., Shima, M., Taniguchi, A., Akagi, M., (2002). 30 mm regeneration of rat sciatic nerve along collagen filaments, *Brain Res. 949* 202-208.

12. Chamberlain, L.J., Yannas, I.V., Hsu, H.P., Strichartz, G., Spector, M., (1998). Collagen-GAG substrate enhances the quality of nerve regeneration through collagen tubes up to level of autograft, *Exp. Neurol, 154* 315-329.

13. Lundborg, G., Dahlin, L., Dohi, D., Kanje, M., Terada, N., (1997). A new type of 'bioartificial' nerve graft for bridging extended defects in nerves, *J. Hand Surg. 22* 299-303.

14. Madison, R.D., Da Silva, C.F., Dikkes, P., (1988). Entubulation repair with protein additives increases the maximum nerve gap distance successfully bridged with tubular prostheses, *Brain Res.* 447 325-334.

15. Meek, M.F., Den Dunnen, W.F.A., Schakenraad, J.M., Robinson, P.H., (1996). Evaluation of functional nerve recovery after reconstruction with a poly(DL-lactide-epsilon-caprolactone) nerve guide, filled modified denatured muscle tissue, *Microsurgery.* 17 555-561.

16. Tong, D.A., Golding, J.P., Edbladh, M., Kroon, M., Ekstrom, A., (1994). Effects of extracellular matrix components on axonal outgrowth from peripheral nerves of adult animals in vitro, *Exp. Neurol.* 146 81-90.

17. Matsumoto, K. et al, (2000). Peripheral nerve regeneration across an 80-mm gap bridged by a polyglycolic acid (PGA)-collagen tube filled with laminin-coated collagen fibers: a histological and electrophysiological evaluation of regenerated nerves, *Brain Res.* 868 315-328.

18. Wen, X., Tresco, P.A., (2006). Effect of filament diameter and extra-cellular matrix molecule precoating on neurite outgrowth and Schwann cell behavior on multifilament entubulation bridging device in vitro, *J Biomed Mater Res.* 76A 626-637.